Published in : Journal of Environmental Management (2025), vol. 375, 124329
DOI: 10.1016/j.jenvman.2025.124329
Status : Postprint (Author's version)

INTEGRATING HIGH-RESOLUTION DATA AND SPECIES-LEVEL TRAITS FOR ENHANCED ECOSYSTEM PROJECTIONS USING A DYNAMIC VEGETATION MODEL: CASE STUDY IN WALLONIA, BELGIUM

Arpita Verma[a,*], Benjamin Lanssens[a], Merja Tölle[c], Ingrid Jacquemin[b], Tarunsinh Chaudhari[a], Alain Hambuckers[d], Louis François[a]

[a] *University of Liege, Department of Astrophysics, Geophysics and Oceanography, SPHERES Research Unit, Belgium*

[b] *University of Liege, Department of Environmental Sciences and Management, SPHERES Research Unit, Belgium*

[c] *Center for Environmental Systems Research, University of Kassel, Germany*

[d] *University of Liege, Biology, Ecology and Evolution Department, SPHERES Research Unit, Belgium*

HANDLING EDITOR:

Jason Michael Evans

KEYWORDS:

Land use change

Carbon sequestration

Regional scale

CARAIB dynamic vegetation model

Climate change

Satellite observation

* **CORRESPONDING AUTHOR** : arpita.verma@uliege.be, arpitaverma08@gmail.com (A. Verma).

ABSTRACT

Accurate quantification of carbon dynamics is critical for developing effective climate mitigation strategies. In this study, we employed the CARAIB dynamic vegetation model (DVM) to analyze carbon fluxes and stocks (biomass and total soil carbon) in Wallonia, Belgium (1980–2070), integrating species-level traits, high- resolution land use/land cover (LULC) data,

Published in : Journal of Environmental Management (2025), vol. 375, 124329
DOI: 10.1016/j.jenvman.2025.124329
Status : Postprint (Author's version)

climate data, and type-1 fuzzy logic for uncertainty quantification. We provide insights into ecosystem resilience and carbon sequestration under Representative Concentration Pathways (RCPs) 2.6 and 8.5. Historical results (1980–2020) demonstrated strong model performance, with gross primary production (GPP) validation achieving R^2 > 0.85 against MODIS and GOSIF datasets, and aboveground biomass correlating well with GEDI (R^2 = 0.77) and ESA-CCI (R^2= 0.91) datasets. Grasslands emerged as critical carbon sinks, exhibiting the highest mean GPP (2480 g C m^{-2} yr^{-1}), surpassing forests due to rapid growth and belowground carbon storage. Future projections (2021–2070) identified afforestation as a robust mitigation strategy, increasing forest GPP by 18% and total biomass by 60–110 Mt C under RCP 8.5. Under RCP 2.6, total biomass was more stable due to the milder emissions trajectory, emphasizing its potential for long-term ecosystem resilience. Interestingly, total soil carbon showed similar levels across both RCPs, indicating belowground carbon resilience despite emissions differences. Sensitivity analyses of LULC scenarios highlighted grassland resilience, with grasslands sustaining a high GPP (2604-2728 g C m^{-2} yr^{-1}) and contributing significantly to soil carbon storage, while deforestation caused substantial carbon losses. These findings underscore the need for nuanced land management, integrating afforestation and grassland conservation, to enhance resilience and sustainable carbon sequestration under climate change.

Introduction

Terrestrial ecosystems are central to the global carbon cycle, exchanging large amounts of carbon with the atmosphere through photosynthesis and respiration (Keenan et al., 2018). Precise estimation of carbon dynamics is essential for advancing climate change mitigation efforts and ensuring sustainable ecosystem management. However, quantifying these fluxes remains challenging (O'Sullivan et al., 2022), particularly at the regional level, because high-resolution data are not often integrated into vegetation models. Gross primary production (GPP), the amount of carbon fixed by plants during photosynthesis, underpins various ecosystem processes, such as respiration, growth, and reproduction (Houghton et al., 2020; Friedlingstein et al., 2023). Net primary productivity (NPP) and net ecosystem productivity (NEP) provide further insights into ecosystem carbon dynamics, with NEP indicating whether an ecosystem acts as a carbon sink or source.

Published in : Journal of Environmental Management (2025), vol. 375, 124329
DOI: 10.1016/j.jenvman.2025.124329
Status : Postprint (Author's version)

At larger scales, net biome productivity (NBP) accounts for disturbances such as fires and human activities, offering a comprehensive measure of net carbon storage (Hari et al., 2022). Given the critical role of carbon fluxes in regulating ecosystem functions and global climate systems, accurate quantification is essential not only for understanding ecosystem processes but also for informing forest management and climate change mitigation efforts (Hong et al., 2021; Junttila et al., 2023). These estimations are vital for maintaining the balance between carbon fluxes and stocks (Jian et al., 2022) and enhancing the reliability of biomass assessments. However, significant challenges persist in assessing carbon dynamics at local and regional scales using modeling approaches (Pongratz et al., 2021). Addressing these challenges requires identifying the factors driving uncertainties in carbon fluxes and leveraging advanced tools like dynamic vegetation models (DVMs) (McGlynn et al., 2022; Trugman et al., 2023).

Wallonia, an ecologically important region in southern Belgium, exemplifies this research gap. Most existing carbon research in Wallonia relies on empirical or observational methods, which, while informative, fall short of addressing uncertainties or predicting ecosystem responses under diverse scenarios (Lettens et al., 2005; Latte et al., 2013; De Wergifosse et al., 2020; Zhou et al., 2022). Applying DVMs to Wallonia's ecosystems is essential to fill this critical gap, providing insights that support regional-scale forest management and climate change mitigation strategies. One such critical driver of uncertainties is land use/land cover (LULC) change, including afforestation, deforestation, and urbanization, which significantly impact the terrestrial carbon balance (Hu et al., 2021; Roebroek et al., 2023).

Given the profound influence of LULC, understanding LULC dynamics is crucial for accurately assessing carbon budgets. Nevertheless, substantial uncertainties remain in quantifying LULC changes and their impacts on carbon dynamics at local and global scales (Pongratz et al., 2021; O'Sullivan et al., 2022; Junttila et al., 2023). To address these challenges, machine learning (ML) techniques offer a promising solution for classifying LULC data from satellite imagery, significantly improving data accuracy (Phan et al., 2020; Yuh et al., 2023). Integrating ML-derived LULC data into DVMs enhances their reliability, enabling better predictions of ecosystem responses to environmental and LULC change (Bastos et al., 2020; Bhan et al., 2021; Bultan et al., 2022; Trugman et al., 2023).

Although significant progress has been made in ecological modeling, vegetation models often

Published in : Journal of Environmental Management (2025), vol. 375, 124329
DOI: 10.1016/j.jenvman.2025.124329
Status : Postprint (Author's version)

lack high-resolution LULC data and species-specific traits, which are crucial for reducing uncertainty in carbon dynamics prediction (Yang et al., 2019). Traits such as stomatal conductance (g0, g1), specific leaf area (SLA), and leaf carbon-to-nitrogen (C:N) ratio play a central role in determining carbon uptake, storage, and release, making them essential for ecosystem modeling (Augusto et al., 2022). Many models still rely on generalized plant functional types (PFTs), limiting their ability to capture species-specific responses to environmental changes (Zakharova et al., 2019).

Incorporating species-specific parameters into process-based ecosystem models, such as dynamic global vegetation models (DGVMs) or terrestrial biosphere models (TBMs), significantly enhances simulation precision and reduces uncertainties in carbon budgets. While these models are predominantly applied at global scales (Jian et al., 2022; O'Sullivan et al., 2022; Friedlingstein et al., 2023), their use at regional scales remains limited. High-resolution simulations that integrate species-level traits and hybrid modeling approaches are essential for bridging this gap (Yang et al., 2019; Li et al., 2021; Bian et al., 2023). Studies that have focused on species-level simulations and regional-scale calibrations (e.g., Dury et al., 2018; Zakharova et al., 2019; Hambuckers et al., 2022) demonstrate the potential for improving model accuracy and producing more reliable carbon budget assessments.

Achieving such improvements necessitates the integration of diverse data sources, including ground-based observations, remote sensing, and statistical datasets, with modeling approaches across spatial and temporal scales (Cai et al., 2020; Bultan et al., 2022; Kong et al., 2022). Among these, satellite-derived data are particularly valuable as they serve as both critical inputs and validation tools, offering detailed insights into biomass, vegetation cover, and productivity (Hunka et al., 2023; Krause et al., 2022; Trugman et al., 2023).

In this study, we aimed to enhance the CARbon Assimilation In the Biosphere (CARAIB) DVM (Gerard et al., 1999; Warnant et al., 1994) by integrating species-level traits, high-resolution LULC data, and climate data to improve the accuracy of regional carbon flux estimates. To achieve these objectives, we first validated the model's accuracy using satellite datasets and ground-based eddy covariance measurements, ensuring reliable ecosystem projections up to 2070. Next, uncertainties in model predictions were quantified based on historical simulations, with strategies developed to minimize these uncertainties in future projections. This involved constraining the model under different climate pathways, using the regional

Published in : Journal of Environmental Management (2025), vol. 375, 124329
DOI: 10.1016/j.jenvman.2025.124329
Status : Postprint (Author's version)

climate model COSMO-CLM aligned with Representative Concentration Pathway (RCP) 8.5 and RCP 2.6. Finally, we evaluated the combined effects of atmospheric CO_2 fertilization and LULC change on ecosystem carbon dynamics, providing actionable insights for climate change mitigation and sustainable land management strategies.

Materials and methods

STUDY REGION

Wallonia, a region in southern Belgium, spans approximately 16,901 km^2, constituting 55% of the country's total land area. It hosts the majority of Belgium's forests, making it a critical region for ecological studies. According to Statbel (https://statbel.fgov.be/en), Wallonia's LULC is diverse, comprising forests (33%), pastures (18%), croplands (25%), and other land types (24%). This varied LULC reflects a balance between natural ecosystems, agricultural areas, and urban development, providing a rich context for exploring regional ecological dynamics and socio-economic interactions (Fig. S1).

CARAIB DVM

The CARAIB DVM was designed to simulate vegetation growth, the carbon balance (Warnant et al., 1994; Gérard et al., 1999), as well as the distribution of vegetation over time (François et al., 1999, 2011; Henrot et al., 2017). Using climatic, atmospheric CO_2, LULC, and species trait data, the model integrates key processes such as soil hydrology, photosynthesis, stomatal regulation (Ball et al., 1987), carbon allocation, and litter–soil dynamics (Hubert et al., 1998; Farquhar et al., 1980; Dury et al., 2018). It includes a crop module for estimating yields based on NPP using a two-stage phenology model (Jacquemin et al., 2020; Loudiyi et al., 2024). The CARAIB DVM has been widely applied to assess climate change impacts on vegetation and carbon sequestration, as well as land management practices (Dury et al., 2011). While effective, the CARAIB DVM has limitations and uncertainties, requiring complementary approaches for a comprehensive understanding.

Further methodological details and input data descriptions are provided in Supplementary Materials section S1.

Published in : Journal of Environmental Management (2025), vol. 375, 124329
DOI: 10.1016/j.jenvman.2025.124329
Status : Postprint (Author's version)

LULC DATA

MAPPING HISTORICAL LULC

We extracted (LULC) information from Landsat satellite data at a 30 m resolution for the period 1985 to 2020. This analysis utilized a composite of Landsat 5, 7, and 8 datasets (Fig. S1), accessed through the Google Earth Engine (GEE) platform to ensure efficient processing and implementation (Gorelick et al., 2017; Amani et al., 2020) (Supplementary Materials section S1.3).

LULC SCENARIOS FOR FUTURE LAND MANAGEMENT

To project LULC changes for 2021–2070, we developed a statistical model based on historical trends (1985–2020) derived from Landsat imagery, classified with ML and validated against ESA CCI data. In Wallonia, historical data show urban expansion with a decline in agricultural land, while forest areas remained stable overall. However, between 2005 and 2020, isolated trees and small vegetation patches declined, while major forests were unaffected. The Landsat-based estimate of 6800 km^2 forest area, including isolated trees, exceeded official records (5600 km^2). Forest dynamics under five scenarios were modeled to assess carbon sequestration and environmental impacts (Figs. S2 (a–e)).

Business as usual.

The business-as-usual (BAU) scenario assumed that the average changes observed during the historical period (1985–2020) will persist into the future (2021–2070). This scenario reflects the continued decline of isolated trees and small patches of vegetation while maintaining the total forest area above the current official estimates. It assumed that the main forest areas remain unaffected throughout the projection period.

Afforestation.

The afforestation scenario was implemented by converting portions of pastureland into forest, resulting in an approximately 35% increase in forest area. The method was applied to randomly selected pasture pixels, ensuring that the fraction of pasture in each selected pixel was never entirely zero. Instead, a portion of the existing pasture fraction was utilized for planting trees, maintaining a balance between afforestation efforts and the preservation of pastureland. This approach evaluated the impacts of pasture-to-forest conversion on

Published in : Journal of Environmental Management (2025), vol. 375, 124329
DOI: 10.1016/j.jenvman.2025.124329
Status : Postprint (Author's version)

ecosystem productivity and carbon sequestration.

Forest shift.
In the forest shift scenario, 20% of forest land was converted to pastureland by 2050, with no urban expansion during this period. Between 2051 and 2070, an additional 20% of forest land was converted directly to urban land. This sequential land conversion allowed for an analysis of the environmental impacts, particularly on ecosystem productivity and carbon sequestration.

Partial deforestation.
In the partial deforestation scenario, forest land was reduced by 20%, with a corresponding increase in urban land. The remaining 80% of the forest remained intact. The term "partial" signifies that while a significant portion of the forest was impacted, not all forest was destroyed nor fully converted to other land uses.

Deforestation.
The deforestation scenario involved the conversion of more than 60% of forest land to urban areas. While it was not complete deforestation, this scenario represented the transformation of a significant portion of forest for urban development. The 60% threshold was considered extensive deforestation, resulting in a near-total loss of forested area.

CLIMATE DATA

The CARAIB DVM requires six meteorological inputs: temperature, precipitation, solar radiation, relative humidity, wind speed, and daily temperature range. Climate data were sourced from the COSMO-CLM (1980–2020), Royal Meteorological Institute (RMI) observations, and GSWP3 for model initialization. Bias correction and validation against RMI data ensured accuracy for historical and future simulations under RCP 8.5 and RCP 2.6. Detailed data processing methodologies are provided in Supplementary Materials section S1.4.

SIMULATION DESIGN

HISTORICAL SIMULATION (1980–2020)

The CARAIB DVM was used to simulate historical ecosystem dynamics at a 1-km resolution, integrating high-resolution datasets to improve accuracy. Inputs included climate variables

Published in : Journal of Environmental Management (2025), vol. 375, 124329
DOI: 10.1016/j.jenvman.2025.124329
Status : Postprint (Author's version)

(1980–2020) from the COSMO-CLM, atmospheric CO_2 (Meinshausen et al., 2011), LULC (1985–2020) from Landsat, soil texture, and species-specific plant parameters. The simulation period (1801–2020) included a spin-up phase to stabilize carbon pools. Outputs such as GPP, NEP, NBP, biomass, and total soil carbon (TSC) provided insights into ecosystem productivity and carbon dynamics under historical conditions. Detailed descriptions of methodologies are provided in Supplementary Materials section S1.5.

INCORPORATING UNCERTAINTY IN PLANT PARAMETERS

In this study, fuzzy logic was applied to address uncertainties in plant physiological parameters, such as stomatal conductance (g_0, g_1), SLA, and the C:N ratio. Triangular fuzzy numbers (TFNs) were used to capture parameter variability, with plausible ranges derived from the TRY database (Kattge et al., 2020) and Miner et al. (2017) (Table S1). Intermediate fuzzy values were calculated for six membership levels (μ = 0 to 1), systematically propagating uncertainty through CARAIB DVM simulations. A detailed explanation of TFNs and parameter calculations is provided in Supplementary Materials section S1.6.

FUTURE SIMULATION (2021–2070)

Future simulations used inputs consistent with historical simulations, including climate variables (Supplement Materials section S1.4), soil texture, and plant physiological parameters, combined with RCP 8.5 and RCP 2.6. These scenarios modeled the impacts of climate change and land-use strategies, including LULC change, as detailed in section 2.3.2, on key ecosystem processes such as carbon sequestration, productivity, and resilience. Output variables (e.g., GPP, NEP, total biomass, and TSC) provided insights into vegetation dynamics and carbon stock changes under contrasting conditions.

VALIDATION

LULC VALIDATION

The accuracy of Landsat-derived LULC classifications (1992–2020) was validated against ESA CCI LULC data (https://planetarycomputer. microsoft.com/dataset/group/esa-cci-lc) harmonized to a 1-km grid for comparison. Misclassification issues, particularly between cropland and pasture, were addressed through selective adjustments, improving consistency and reliability. Further details are provided in Supplementary Materials section S1.7.

Published in : Journal of Environmental Management (2025), vol. 375, 124329
DOI: 10.1016/j.jenvman.2025.124329
Status : Postprint (Author's version)

CLIMATE DATA VALIDATION

The COSMO-CLM outputs (1980–2020) were validated against RMI observational data (Journee et al., 2023) using metrics such as bias, standard deviation, and root mean square error (RMSE). Model outputs were upscaled to match the 5-km resolution of observations. Detailed validation procedures and results are provided in Supplementary Materials section S1.8.

CARAIB DVM VALIDATION

The accuracy of the CARAIB DVM was validated using MODIS and GOSIF datasets for GPP over the period 2001–2020, and ESA-CCI and GEDI datasets for AGB in 2020. Regression analyses, quantified by R^2 and RMSE, and geographically weighted regression (GWR) were used to assess agreement between modeled and observed values, highlighting regional discrepancies and areas for model improvement. Further details on the validation methodology are provided in Supplementary Materials section S1.9.

Results

INPUT DATA VALIDATION

LULC DATA

The validation of LULC data demonstrated strong agreement between Landsat-derived classifications and the harmonized ESA CCI dataset over the Wallonia region (1992–2020), with an average accuracy of 88% and substantial agreement reflected in kappa coefficients. Yearly trends in accuracy and kappa coefficients are presented in the Supplementary Materials (Section S2.1, Fig. S3).

CLIMATE DATA

The COSMO-CLM was validated against RMI observational data (1980–2020) for precipitation, temperature, relative humidity, solar radiation, and wind speed. The model demonstrated strong performance for temperature, with low bias and RMSE, capturing seasonal trends effectively. However, precipitation was consistently overestimated in wetter months and underestimated in drier periods, with challenges in representing extremes. Relative humidity and solar radiation exhibited seasonal discrepancies, particularly during summer, with solar radiation consistently overestimated. Wind speed showed the highest variability, with

Published in : Journal of Environmental Management (2025), vol. 375, 124329
DOI: 10.1016/j.jenvman.2025.124329
Status : Postprint (Author's version)

systematic overestimation across most months. These findings underscore the model's reliability in temperature simulation and its limitations in accurately capturing extremes and variability for other meteorological variables (Supplementary Materials section S2.2, Fig. S4).

HISTORICAL RESULTS WITH VALIDATION

MODEL ADVANCEMENT USING HIGH-RESOLUTION INPUT DATA AND SPECIES-LEVEL TRAITS

The CARAIB DVM was improved by incorporating a species-level trait-based approach and integrating high-resolution LULC and climate data. The inclusion of species-specific traits, such as SLA, height (h0), and growth rates, allowed the model to simulate carbon dynamics across various species and LULC types with greater accuracy. This advancement markedly improved the estimations of carbon fluxes (GPP, NEP, and NBP) and carbon stocks in Wallonia, offering deeper insights into regional carbon dynamics.

Among the six major LULC classes in the model, forests, crops, and pastures were identified as particularly significant for carbon sequestration (Fig. 1a). Grasslands demonstrated a high mean GPP of 2480 g C m^{-2} yr^{-1} due to their extensive root systems and rapid growth rates, outperforming forests and croplands, which exhibited mean GPP values of 1312 and 990 g C m^{-2} yr^{-1}, respectively (Fig. 1b). These differences highlight the varying photosynthetic efficiencies and ecosystem dynamics across LULC types.

NEP showed significant regional variability, particularly in forests and pastures, with simulated mean values of 73 and 12 g C m^{-2} yr^{-1}, respectively, indicating their roles as net carbon sinks (Fig. 1c). Croplands had a higher NEP, averaging 111 g C m^{-2} yr^{-1}. The mean NBP of forests was notably high, averaging 59 g C m^{-2} yr^{-1}, underscoring their importance as major carbon sinks. In contrast, pastures exhibited a mean NBP of -19 g C m^{-2} yr^{-1}, while croplands displayed a lower mean NBP of -34 g C m^{-2} yr^{-1}, likely due to regular harvesting practices that remove biomass (Fig. 1d). These mean NEP and NBP values were calculated based on the dominant LULC class within each pixel.

In the model, litter production from all plant types was combined into a single reservoir of leaf or woody litter to simplify the estimation of heterotrophic respiration at the pixel level. This approach avoided complexities related to variations in plant species or LULC types. By streamlining the process, the model ensured more consistent carbon exchange estimates,

Published in : Journal of Environmental Management (2025), vol. 375, 124329
DOI: 10.1016/j.jenvman.2025.124329
Status : Postprint (Author's version)

determined primarily by the dominant LULC type in each pixel. As a result, the accuracy of NEP and NBP as indicators of carbon dynamics relies significantly on precise LULC classification, which governs the main carbon exchange processes.

VALIDATION OF MODEL OUTPUTS

GPP: validation against satellite observations.

To further evaluate the accuracy of our results, we compared the model's output with satellite-derived GPP (Fig. 2).

Spatial regression: A significantly high local R^2 of 0.85 between CARAIB DVM-derived GPP and MODIS-derived GPP (mean for 2001–2020) at a 1-km^2 resolution demonstrated the ability of the CARAIB DVM to capture spatial heterogeneity across the landscape (Fig. 2b–d). When comparing the distribution of CARAIB DVM-derived and GOSIF-derived mean GPP at the GOSIF scale (0.05°), we achieved an even higher local R^2 of 0.97, further validating the model's ability to reproduce spatial patterns (Fig. 2e–g).

Linear regression: Linear regression between MODIS-derived and CARAIB DVM-derived annual GPP indicated high performance, yielding global R^2 values ranging from 0.50 to 0.65 (Fig. S6a). Similarly, there was as strong global correlation between GOSIF-derived and CARAIB DVM-derived annual GPP, with R^2 values ranging from 0.36 to 0.74 (Fig. S6b).

GPP: eddy covariance correlation analysis.

Fig. S7a presents a time series of GPP at the BE-Vielsalm eddy-covariance station (50.31°N, 5.99°E), showing a comparison among GPP estimates from eddy covariance data (GPP_EC), MODIS (GPP_MOD), and CARAIB DVM (GPP_CARAIB) for 1996–2014. The close temporal alignment among these datasets demonstrates the model's capability to capture seasonal and interannual variations in GPP. For managed pasture systems, Fig. S7b highlights GPP comparisons at the BE-Dorinne eddy-covariance station (50.30°N, 4.93°E). While the CARAIB DVM slightly overestimates GPP, with values ranging from 2384 to 2542 g C m^{-2} yr^{-1}, the results remain comparable to eddy covariance measurements (2024-2357 g C m^{-2} yr^{-1}; Gourlez De La Motte et al., 2016) for 2011–2014. This analysis emphasizes the model's reliability across diverse LULC types while identifying areas for fine-tuning.

AGB estimates.

The comparison of AGB estimates derived from the CARAIB DVM and from ESA-CCI and GEDI

Published in : Journal of Environmental Management (2025), vol. 375, 124329
DOI: 10.1016/j.jenvman.2025.124329
Status : Postprint (Author's version)

revealed significant alignment, further validating the accuracy of the model-derived estimates.

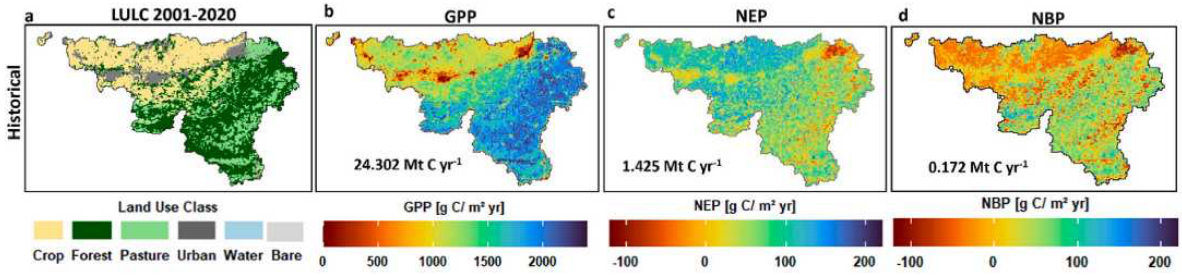

Fig. 1. Comparative analysis of mean LULC and carbon fluxes (ecosystem productivity) for the years 2001–2020. (a) Landsat-derived historical LULC; (b) CARAIB DVM-derived GPP (g C m-2 yr-1); (c) CARAIB DVM-derived NEP (g C m-2 yr-1); (d) CARAIB DVM-derived NBP (g C m-2 yr-1). The values represent cumulative fluxes over Wallonia, with NEP and NBP being positive when the ecosystem acts as a carbon sink for the atmosphere.

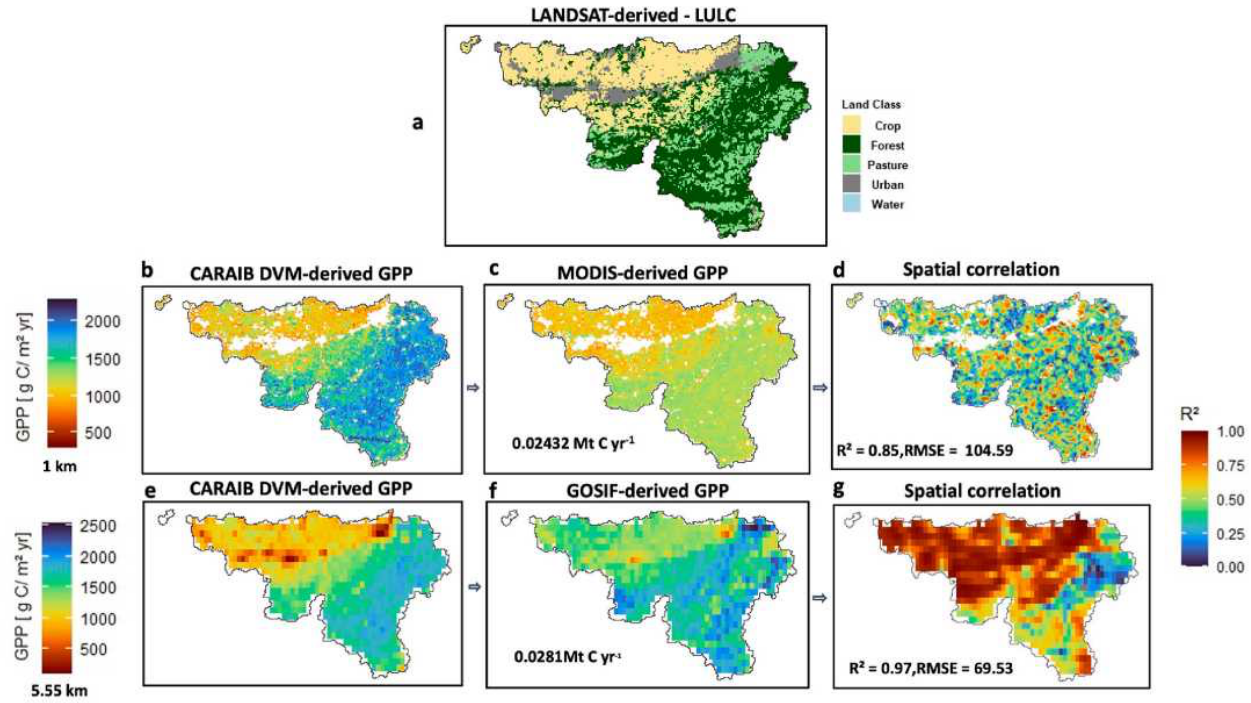

Fig. 2. Map of mean GPP (2001–2020) from CARAIB DVM, MODIS, and GOSIF, with spatial correlations between model and satellite data. (a) Landsat-derived historical LULC. (b–d) Spatial correlation between CARAIB DVM-derived and MODIS-derived mean GPP (resolution: 1 km). (e–g) Spatial correlation between CARAIB DVM-derived and GOSIF-derived mean GPP (resolution: 5.55 km). R2 and RMSE values were computed using a geographically weighted regression method.

Published in : Journal of Environmental Management (2025), vol. 375, 124329
DOI: 10.1016/j.jenvman.2025.124329
Status : Postprint (Author's version)

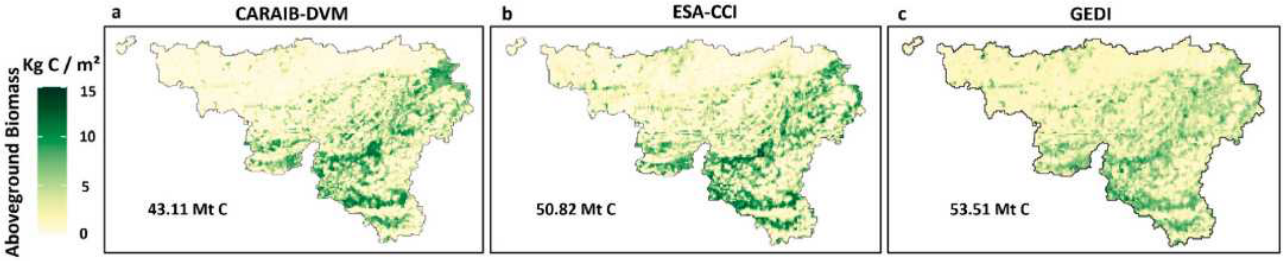

Fig. 3. Spatial distribution of aboveground biomass in 2020 as estimated by the CARAIB DVM, ESA-CCI and GEDI. The number in each plot is the total aboveground biomass over the Wallonia region.

Fig. 3a-c shows the spatial distribution of AGB for 2020 estimated by the CARAIB DVM, ESA-CCI, and GEDI. Fig. S8a highlights a strong spatial correlation between CARAIB DVM-derived AGB and ESA-CCI- derived AGB (local R^2 = 0.91), while Fig. S8d presents a scatter plot with an R^2 of 0.75 and RMSE of 1.56 kg C/m^2, indicating a strong positive correlation with some discrepancies. Similarly, the comparison between CARAIB DVM-derived AGB and GEDI-derived AGB (Fig. S8b) yielded a local spatial R^2 of 0.77 and a scatter plot R^2 of 0.56, with an RMSE of 1.41 kg C/m^2 (Fig. S8e), reflecting reasonable agreement but notable deviations.

Comparative analysis among GEDI, CARAIB DVM, and ESA-CCI datasets revealed moderate correlations. The R^2 values of 0.56 for both GEDI vs. CARAIB DVM and GEDI vs. ESA-CCI (Figs. S8c and S8f) indicate these models explain approximately 56% of the variance in the GEDI dataset. The similar RMSE values of 1.41 kg C/m^2 (GEDI vs. CARAIB DVM) and 1.43 kg C/m^2 (GEDI vs. ESA-CCI) highlight comparable average errors, though persistent discrepancies remain between model estimates and satellite-derived data.

LULC AS A PREDICTOR OF TERRESTRIAL CARBON BALANCE IN THE FUTURE (2021–2070)

This study investigated the effects of future climate pathways and LULC scenarios on ecosystem productivity and carbon dynamics in Wallonia. Two climate pathways were analyzed: RCP 8.5 (high emissions) and RCP 2.6 (low emissions). The focus was on carbon fluxes (GPP, NPP, and NBP) and carbon stocks (total biomass and TSC) under two primary LULC scenarios: a baseline scenario (BAU), which assumes a continuation of current LULC practices, and an afforestation scenario, where grasslands are converted to forest to increase forest cover.

Published in : Journal of Environmental Management (2025), vol. 375, 124329
DOI: 10.1016/j.jenvman.2025.124329
Status : Postprint (Author's version)

For sensitivity analysis, these scenarios are compared against three hypothetical deforestation scenarios: forest shift (conversion of forests to grassland and urban land), partial deforestation (moderate reduction in forest cover), and deforestation (extensive removal of forest cover). Carbon dynamics were assessed across two time periods, 2021–2045 and 2046–2070, to evaluate both near-term and mid-term impacts.

MAIN LULC SCENARIOS

Two main LULC scenarios (BAU and afforestation) were analyzed under two climate pathways (RCP 2.6 and RCP 8.5), focusing on key indicators of ecosystem productivity.

Carbon sequestration.

Under RCP 2.6, the BAU scenario was estimated to have a mean GPP of 1430 g C m^{-2} yr^{-1} during 2021–2045, decreasing slightly to 1412.8 g C m^{-2} yr^{-1} by 2046–2070. Forest mean GPP showed a modest increase from 1520.6 to 1670.3 g C m^{-2} yr^{-1}, while pasture mean GPP remained consistently high, increasing from 2483.6 to 2498.1 g C m^{-2} yr^{-1}. In the afforestation scenario, overall mean GPP decreased slightly; however, forest mean GPP increased to 1600.4 g C m^{-2} yr^{-1}, while pasture productivity remained stable (Fig. 4, Fig. S9a). Similarly, under RCP 8.5, the BAU mean GPP increased from 1421.4 to 1474.8 g C m^{-2} yr^{-1}, with forest mean GPP rising significantly from 1435.4 to 1644.6 g C m^{-2} yr^{-1}.

In the afforestation scenario, pasture mean GPP also showed notable gains, increasing from 2608.2 to 2747.5 g C m^{-2} yr^{-1}, primarily driven by elevated CO_2 levels. Forest mean GPP further increased under afforestation, rising from 1368 to 1553 g C m^{-2} yr^{-1}, underscoring the enhanced carbon sequestration potential of reforested landscapes.

Further, under RCP 2.6, the BAU scenario was estimated to have a mean NEP of 85 g C m^{-2} yr^{-1} during 2021–2045, declining to 53.14 g C m^{-2} yr^{-1} by 2046-2070 (Figs. S9b-c). Correspondingly, mean NBP decreased from 22.69 to -11.78 g C m^{-2} yr^{-1}, reflecting reduced carbon sequestration as conditions worsened over time. In contrast, under RCP 8.5, the BAU scenario showed lower sequestration potential, with mean NEP declining from 62.75 to 54.71 g C m^{-2} yr^{-1} across the same periods. NBP also transitioned from a marginally positive 0.36 to -11.32 g C m^{-2} yr^{-1}, indicating net carbon losses under more extreme climatic conditions.

The afforestation scenario, however, demonstrated a stronger sequestration capacity. Under RCP 2.6, mean NEP improved to 92.04 g C m^{-2} yr^{-1} during 2021–2045 and remained high at 87.63

Published in : Journal of Environmental Management (2025), vol. 375, 124329
DOI: 10.1016/j.jenvman.2025.124329
Status : Postprint (Author's version)

g C m^{-2} yr^{-1} during 2046–2070, while NBP increased from 32.02 to 27.95 g C m^{-2} yr^{-1}. Similarly, under RCP 8.5, afforestation increased NEP from 68.41 to 88.17 g C m^{-2} yr^{-1}, with NBP rising from 7.53 to 27.4 g C m^{-2} yr^{-1}. These findings highlight the importance of afforestation in mitigating carbon losses under both climate pathways, particularly in contrast to the declines observed in the BAU scenario under these pathways.

Spatial distribution of carbon sequestration in RCP 8.5.

After comparing overall carbon dynamics between RCP 2.6 and RCP 8.5, we focused on determining the spatial distributions of GPP, NEP, and NBP under the BAU and afforestation scenarios for the periods 2021–2045 and 2046–2070 under RCP 8.5 (Fig. 5). In the BAU scenario, GPP was higher in forested regions, particularly in the southern areas, while NEP and NBP displayed localized carbon losses in urban and pasture- dominated areas. In contrast, the afforestation scenario expands forest cover, leading to enhanced GPP and reduced carbon loss hotspots across the region. By 2046–2070, afforestation markedly increased NEP and NBP, particularly in the central and southern regions, underscoring its potential to enhance carbon sequestration under future high-emission pathways.

Carbon stocks

Under the BAU scenario, total biomass increased for 2021–2045 under RCP 2.6, reaching higher levels compared to that under RCP 8.5 (80 Mt C). For 2046–2070, total biomass under RCP 2.6 showed a significant increase, highlighting improved long-term carbon sequestration potential, while total biomass under RCP 8.5 remained relatively stable (Fig. 6a-b). In the afforestation scenario, total biomass rose substantially (110 Mt C) for 2021–2045 under RCP 2.6, with slightly lower gains under RCP 8.5. For 2046–2070, both scenarios showed further increases, with RCP 2.6 exhibiting the highest total biomass values. In the BAU and afforestation scenarios, TSC remained stable for both periods (270 Mt C) under RCP 2.6 and RCP 8.5, indicating limited sensitivity to climate pathways (Fig. 6c–d).

SENSITIVITY ANALYSIS

A sensitivity analysis was conducted to evaluate changes in carbon sequestration under different LULC scenarios and climate pathways. The scenarios analyzed included forest shift, partial deforestation, and deforestation. These scenarios were designed to assess the impacts of varying levels of forest cover reduction and LULC changes on carbon dynamics under two climate pathways, RCP 8.5 (high emissions) and RCP 2.6 (low emissions). The results highlight

Published in : Journal of Environmental Management (2025), vol. 375, 124329
DOI: 10.1016/j.jenvman.2025.124329
Status : Postprint (Author's version)

the trends observed for each scenario, providing insights into the potential consequences of land-use decisions in the context of different climate change projections.

Carbon sequestration.

In the forest shift scenario, mean GPP under RCP 2.6 increased slightly from 1481 to 1489 g C m^{-2} yr^{-1} (2021–2045 vs. 2046–2070), with forest mean GPP rising from 1574 to 1761 g C m^{-2} yr^{-1} and pasture mean GPP increasing marginally from 2485 to 2499 g C m^{-2} yr^{-1}. Similarly, under RCP 8.5, mean GPP increased from 1481 to 1565 g C m^{-2} yr^{-1}, with significant increases in pasture productivity (2519–2656 g C m^{-2} yr^{-1}). In the later period (2051–2070), urban expansion reduced overall productivity, but remaining forests demonstrated resilience with forest GPP increasing from 1473 to 1756 g C m^{-2} yr^{-1}. However, the overall yearly cumulative GPP decreased from 2050 to 2070 (Fig. 4a–b, Fig. S10a).

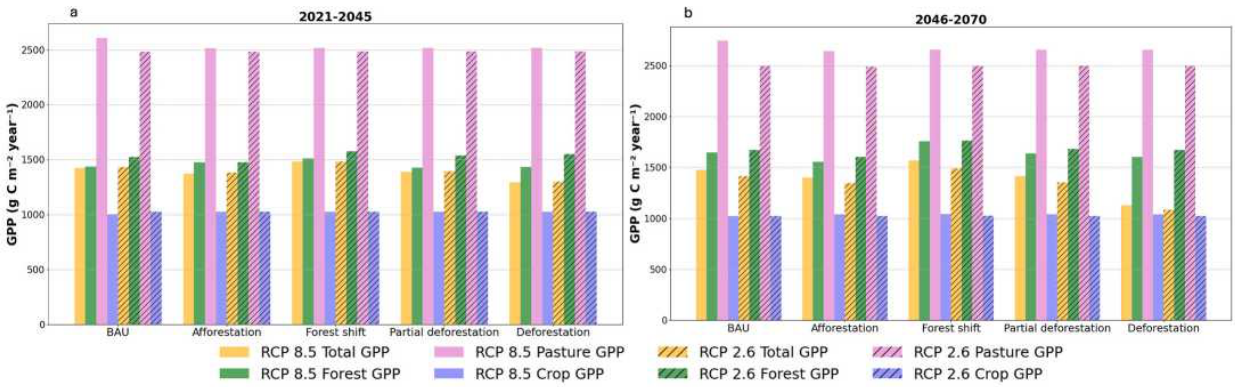

Fig. 4. Spatially aggregated GPP (g C m-2 y-1) under different LULC scenarios and climate pathways. (a) GPP for 2021-2045. (b) GPP for 2046-2070. Contributions from total GPP, forest GPP, pasture GPP, and crop GPP are shown across BAU, afforestation, forest shift, partial deforestation, and deforestation scenarios under RCP 8.5 (solid bars) and RCP 2.6 (striped bars).

Published in : Journal of Environmental Management (2025), vol. 375, 124329
DOI: 10.1016/j.jenvman.2025.124329
Status : Postprint (Author's version)

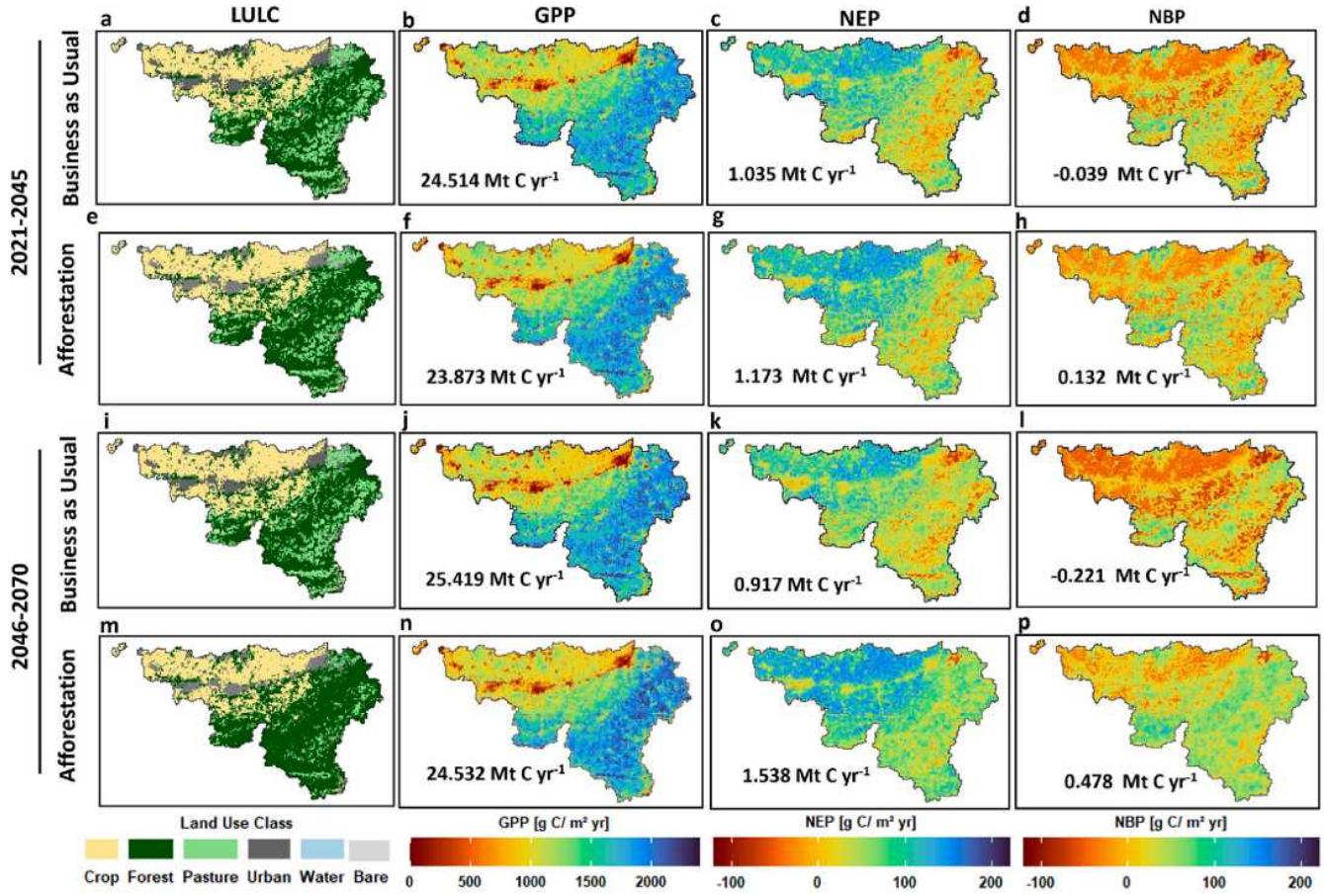

Fig. 5. Comparative analysis of LULC and carbon fluxes (ecosystem productivity) in two observation cycles (2021–2045, 2047–2070), evaluating the impact of BAU (5a-d, 5i-l) and afforestation (5e-h, 5m-p) scenarios. The number appearing in each plot is the cumulative flux over the Wallonia region.

In the partial deforestation scenario, mean GPP under RCP 2.6 remained stable (1391–1351 g C m^{-2} yr^{-1}), with a modest increase in forest GPP (1536–1680 g C m^{-2} yr^{-1}) and pasture GPP (2484–2500 g C m^{-2} yr^{-1}). Similarly, under RCP 8.5, GPP rose from 1384 to 1412 g C m^{-2} yr^{-1}, with forest GPP increasing from 1426 to 1634 g C m^{-2} yr^{-1} and pasture GPP from 2518 to 2657 g C m^{-2} yr^{-1} (Fig. 4a–b, Fig. S10d). In contrast, in the deforestation scenario, mean GPP under RCP 2.6 declined significantly from 1296 to 1086 g C m^{-2} yr^{-1}, while under RCP 8.5, it dropped from 1290 to 1133 g C m^{-2} yr^{-1}. Despite these declines, pasture GPP increased slightly in both scenarios (Fig. 4a–b, Fig. S10g).

In the forest shift scenario, under RCP 2.6, mean NEP decreased from 68.3 g C m^{-2} yr^{-1} during 2021–2045 to 7.56 g C m^{-2} yr^{-1} by 2046–2070, while NBP dropped sharply from 8.25 to -52.24 g C m^{-2} yr^{-1}. Under RCP 8.5, mean NEP followed a similar trend, decreasing from 52.92 to 10.32 g C m^{-2} yr^{-1}, with mean NBP declining from -6.82 to -50.55 g C m^{-2} yr^{-1}. In the partial deforestation

Published in : Journal of Environmental Management (2025), vol. 375, 124329
DOI: 10.1016/j.jenvman.2025.124329
Status : Postprint (Author's version)

scenario, under RCP 2.6, mean NEP declined from 72.41 to 35.69 g C m^{-2} yr^{-1}, while NBP dropped from 12.39 to -24.05 g C m^{-2} yr^{-1}. Under RCP 8.5, NEP decreased from 51.21 to 37.46 g C m^{-2} yr^{-1}, and NBP showed a larger decline, from -8.49 to -23.36 g C m^{-2} yr^{-1}.

In the deforestation scenario, both mean NEP and mean NBP exhibited the most severe declines. Under RCP 2.6, mean NEP dropped from 44.37 g C m^{-2} yr^{-1} during 2021–2045 to -8.34 g C m^{-2} yr^{-1} by 2046–2070, while mean NBP declined from -15.64 to -68.1 g C m^{-2} yr^{-1}. Similarly, under RCP 8.5, NEP turned negative, decreasing from 28 to -6.21 g C m^{-2} yr^{-1}, with NBP dropping sharply from -31.69 to -67.54 g C m^{-2} yr^{-1}. These trends underline the devastating consequences of forest loss, with ecosystems transitioning from carbon sinks to sources.

Spatial distribution of carbon sequestration in RCP 8.5.

The spatial maps (Fig. 7a–l, 8a-l) highlight the impacts of LULC scenarios on GPP, NEP, and NBP across 2021–2045 and 2046–2070. These maps show distinct spatial patterns of carbon sequestration under forest loss and urban expansion. In the forest shift scenario, sustained GPP was observed in forested and grassland regions, but NEP and NBP showed substantial spatial declines, with some areas transitioning to a net carbon loss by 2046–2070 (Fig. 7a–d, 8a-d). In the partial deforestation scenario, stable GPP persisted in forested areas, but fragmentation led to localized carbon losses in NEP and NBP, becoming more pronounced by 2046–2070 (Fig. 7e–h, 8e-h). The deforestation scenario showed the most severe impacts, with widespread declines in GPP and carbon losses across the region. NEP and NBP transitioned to predominantly negative values, reflecting near-complete forest-to-urban conversion (Fig. 7i–l, 8i-l).

Carbon stocks.

Under the forest shift scenario, total biomass increased moderately under RCP 2.6 during 2021–2045 and remained higher than that under RCP 8.5 in 2046–2070, reflecting milder climate conditions. In the partial deforestation scenario, total biomass declined significantly under both RCPs compared to BAU, with larger declines under RCP 8.5, particularly in 2046–2070, due to harsher climate conditions. The deforestation scenario resulted in the lowest total biomass levels across all periods, with marginally higher values under RCP 2.6, emphasizing the severe impacts of forest loss. In contrast, TSC exhibited much smaller variations across all scenarios compared to total biomass, despite its larger overall stock. RCP 2.6 generally maintained slightly higher TSC levels than RCP 8.5. Even under deforestation,

Published in : Journal of Environmental Management (2025), vol. 375, 124329
DOI: 10.1016/j.jenvman.2025.124329
Status : Postprint (Author's version)

TSC declines were less pronounced under RCP 2.6, highlighting the stability and resilience of TSC compared to total biomass.

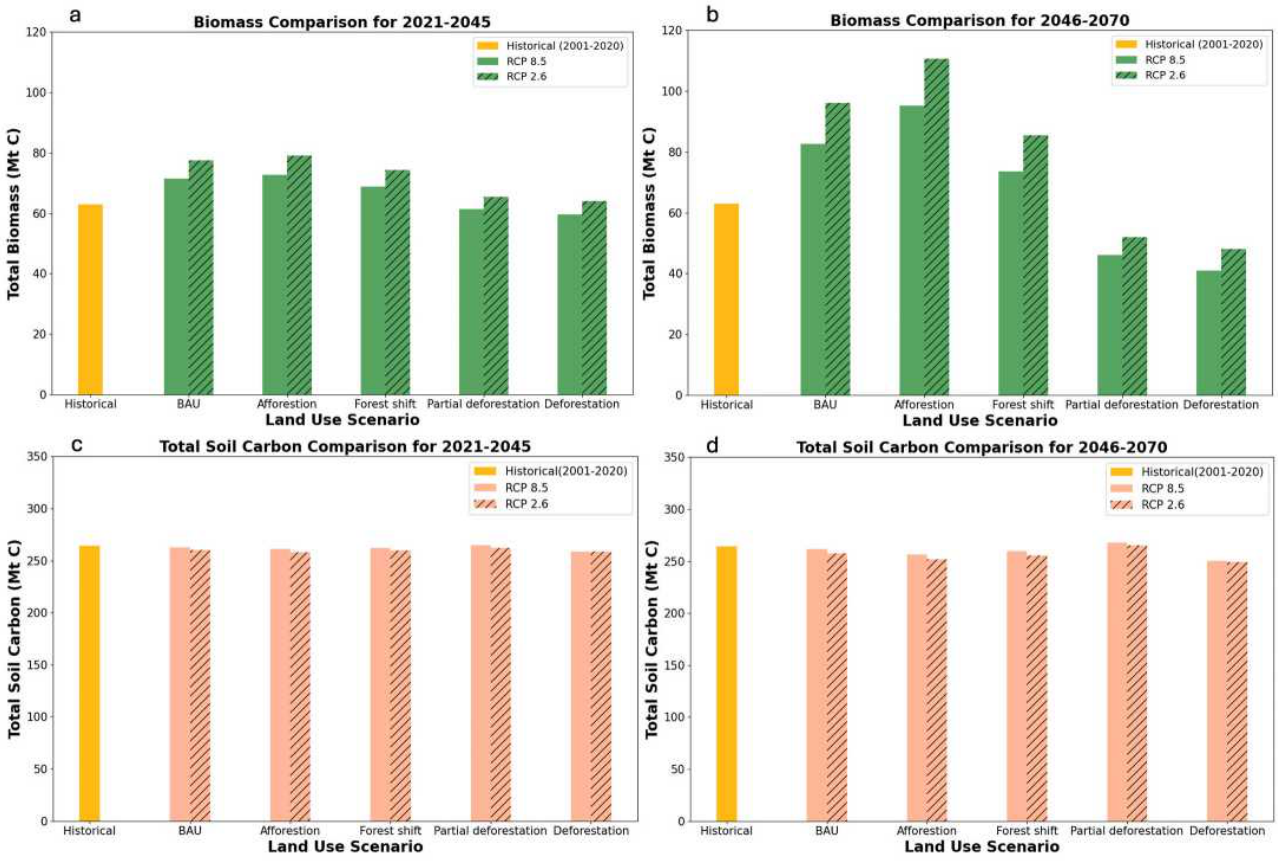

Fig. 6. Comparison of total biomass and total soil carbon across LULC scenarios for 2021–2045 and 2046–2070. (a–b) represent biomass for 2021–2045 and 2046–2070, respectively, while (c–d) illustrate total soil carbon for the same periods.

MODEL UNCERTAINTY ANALYSIS

The uncertainty in model predictions for GPP, NEP, total biomass, and TSC was evaluated using fuzzy membership levels (left, peak, and right) for the period 1980–2020 over 20 grid cells of various representative LULC classes. Variability was quantified by calculating the mean and standard deviation (SD) across fuzzy simulations. To represent uncertainty, a range defined at the 90% confidence level was derived. This range indicates the interval within which the true mean is expected to lie with 90% confidence, capturing the variability introduced by uncertainties in key plant physiological parameters, such as g_0, g_1, SLA and C:N.

Published in : Journal of Environmental Management (2025), vol. 375, 124329
DOI: 10.1016/j.jenvman.2025.124329
Status : Postprint (Author's version)

The mean GPP was 1875 g C m^{-2} yr^{-1}, with an SD of 148 g C m^{-2} yr^{-1}, resulting in an uncertainty range of ±243 g C m^{-2} yr^{-1}. GPP exhibited substantial variability across fuzzy membership levels, with higher estimates for left-side memberships and lower estimates for right-side memberships (Fig. S11a). NEP had a mean value of 82 g C m^{-2} yr^{-1}, with an SD of 14 g C m^{-2} yr^{-1} and an uncertainty range of ±23 g C m^{-2} yr^{-1}. NEP predictions ranged from net carbon gains to near-neutral or negative fluxes across membership levels (Fig. S11b). Total biomass showed a mean value of 10.41 kg C m^{-2} yr^{-1}, with an SD of 1.51 kg C m^{-2} yr^{-1} and an uncertainty range of ±2.49 kg C m^{-2} yr^{-1}, while TSC had a mean of 20.06 kg C m^{-2} yr^{-1}, an SD of 1.68 kg C m^{-2} yr^{-1}, and an uncertainty range of ±2.76 kg C m^{-2} yr^{-1}. Total biomass remained stable across fuzzy membership levels, whereas TSC exhibited minimal variability, reflecting its resilience as a long-term carbon pool (Figs. S12a and S12b).

Discussion

The results of this study provide valuable insights into the role of high-resolution inputs and species-specific traits in enhancing the predictive accuracy of vegetation models like the CARAIB DVM. By validating model inputs and outputs against observed and satellite data, we demonstrated the reliability of the CARAIB DVM in simulating regional carbon dynamics. This discussion explores the implications of our findings in the context of existing literature, emphasizing the importance of integrating accurate data and robust sensitivity analyses to inform climate mitigation strategies (O'Sullivan et al., 2022; Pongratz et al., 2021; Trugman et al., 2023; Friedlingstein et al., 2023). Key areas of the discussion include the integration of high-resolution inputs, uncertainty analysis, validation of model outputs, and the implications of future LULC scenarios.

INTEGRATION OF HIGH-RESOLUTION INPUTS AND SPECIES-SPECIFIC TRAITS

The integration of high-resolution LULC and climate datasets, coupled with species-specific traits, significantly enhanced the CARAIB DVM's ability to simulate carbon dynamics in Wallonia, Belgium. Validation of LULC datasets demonstrated strong reliability, achieving accuracy levels between 88% and 92% with robust kappa coefficients. This effectively resolved classification challenges, particularly in distinguishing crops and pastures, which are

Published in : Journal of Environmental Management (2025), vol. 375, 124329
DOI: 10.1016/j.jenvman.2025.124329
Status : Postprint (Author's version)

often difficult to differentiate in remote sensing-based classifications (Li et al., 2018; García-Alvarez et al., 2022). Similarly, validation of climate data against RMI observations confirmed minimal biases and low RMSE, ensuring the accuracy and reliability of these datasets as inputs for carbon flux and stock simulations (Journee and Bertrand, 2011; Journee et al., 2023). These robust inputs allowed the CARAIB DVM to accurately capture carbon dynamics across diverse LULC types.

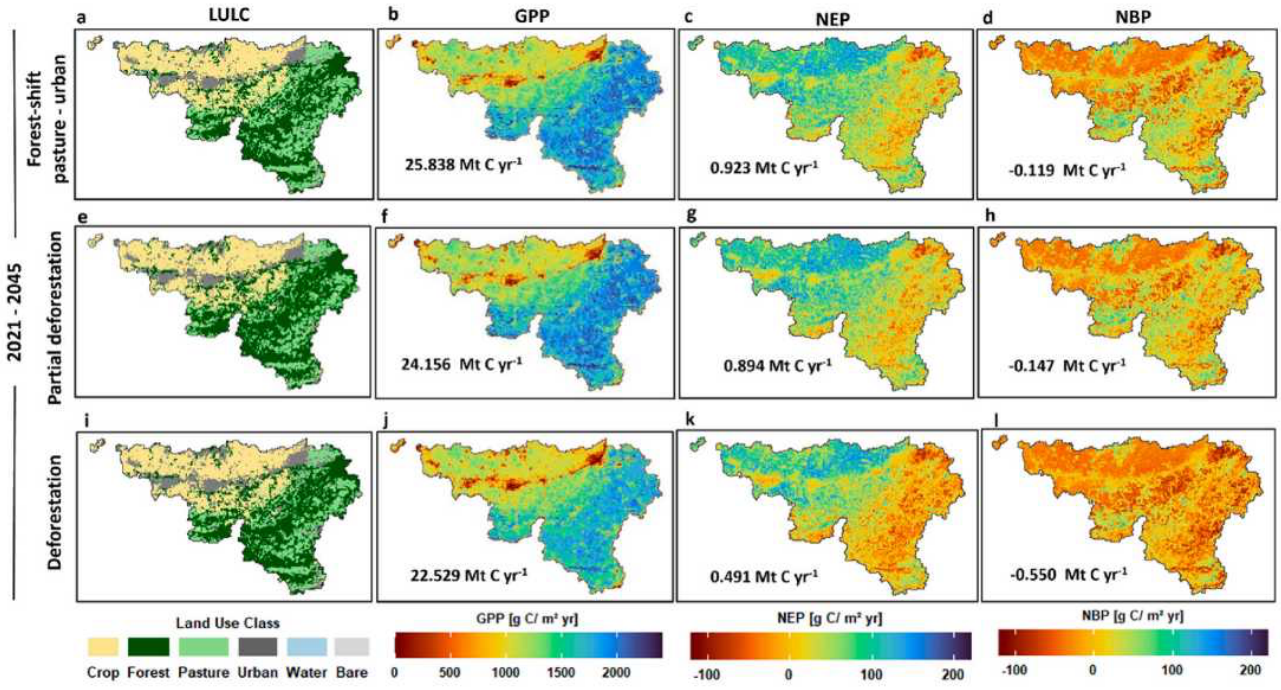

Fig. 7. Sensitivity analysis of LULC change and its impact on mean ecosystem productivity in 2021–2045. (a–d) Forest shift scenario. (e–h) Partial deforestation scenario. (i–l) Deforestation scenario. The number appearing in each plot is the cumulative flux over the Wallonia region.

Published in : Journal of Environmental Management (2025), vol. 375, 124329
DOI: 10.1016/j.jenvman.2025.124329
Status : Postprint (Author's version)

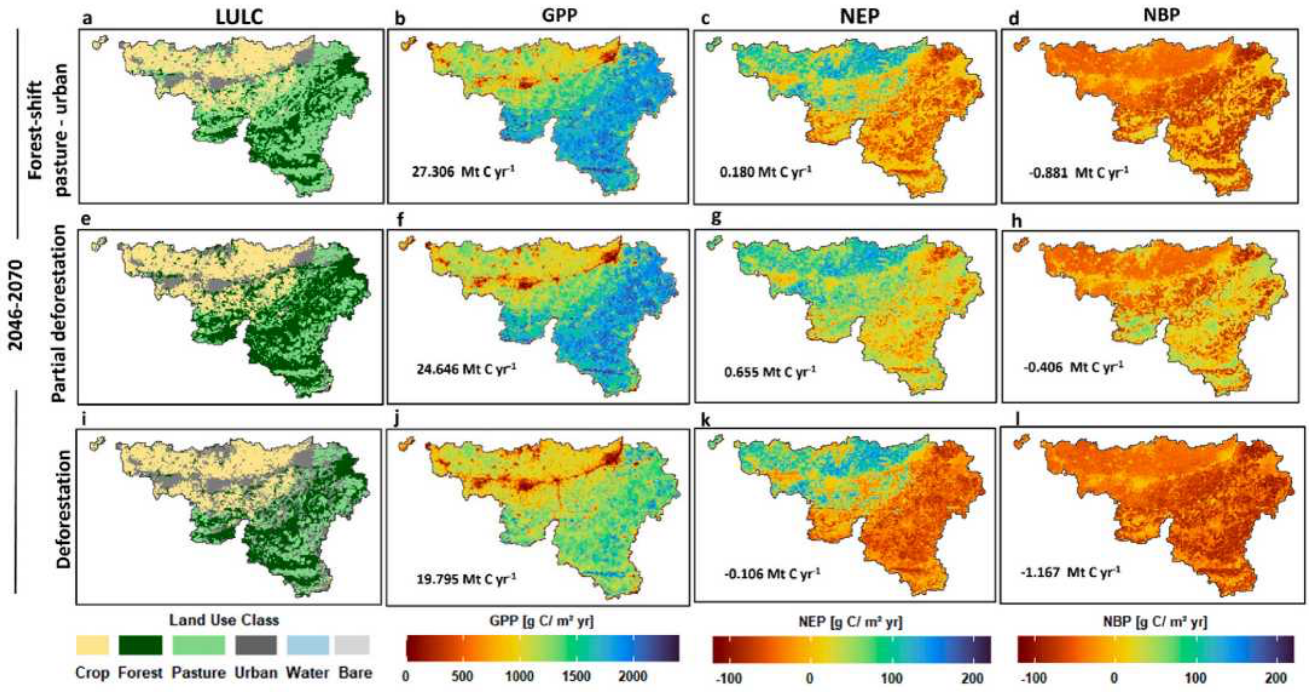

Fig. 8. Sensitivity analysis of LULC change and its impact on mean ecosystem productivity in 2046–2070. (a–d) Forest shift scenario. (e–h) Partial deforestation scenario. (i–l) Deforestation scenario. The number appearing in each plot is the cumulative flux over the Wallonia region.

Contrary to global-scale findings (Krause et al., 2022), at the local scale, pasture (grassland) was more productive than the other two ecosystems (forest and cropland, Fig. 1b) (Guo et al., 2002; Zhao et al., 2023). On a global scale, natural grasslands are found in more arid and less productive areas compared to forests. However, in regions like Wallonia, pastures have replaced natural forests following historical deforestation and thus appear in much wetter areas adjacent to forests. Unlike forest trees, pasture species are not deciduous and do not need to sustain a large biomass through respiration, allowing their growth rate to respond more quickly to warming in the spring, which in turn enhances photosynthesis efficiency throughout the year (Dass et al., 2018; Rojas-Botero et al., 2023). Net carbon fluxes also showed notable variation among LULC types, with forests acting as strong carbon sinks (mean NBP: 59 g C m^{-2} yr^{-1}), while croplands and pastures exhibited net carbon losses (-34 and -19 g C m^{-2} yr^{-1}, respectively).

These results highlight the critical role of land management practices, such as harvesting and grazing, in influencing carbon dynamics (Prescher et al., 2010). These findings set the foundation for validating CARAIB DVM outputs and exploring the model's applicability across diverse scenarios.

Published in : Journal of Environmental Management (2025), vol. 375, 124329
DOI: 10.1016/j.jenvman.2025.124329
Status : Postprint (Author's version)

VALIDATION OF MODEL OUTPUTS

The CARAIB DVM demonstrated strong accuracy in simulating carbon fluxes when validated against satellite-derived datasets (MODIS, GOSIF) and eddy covariance data from Fluxnet sites. At the spatial scale, the model achieved an R^2 of 0.85 with MODIS GPP at a 1-km^2 resolution and 0.97 with GOSIF at a 5.55-km resolution (Li et al., 2019), effectively capturing spatial heterogeneity. Temporal validation further confirmed the model's reliability across various LULC types, including managed pastures. AGB estimates also showed strong alignment with ESA-CCI (R^2 = 0.91) and GEDI (R^2 = 0.77) datasets, showcasing the model's ability to represent AGB distribution accurately (Duncanson et al., 2019; Hunka et al., 2023).

Comparisons between CARAIB DVM-derived GPP and satellite data revealed consistent trends, despite minor biases. MODIS slightly underestimated GPP values, likely due to LAI representation differences (Bian et al., 2023), while GOSIF overestimated GPP values in certain regions, reflecting potential discrepancies in light-use efficiency models (Sun et al., 2017).

Moreover, temporal alignment with Fluxnet sites, such as Vielsalm (Tang et al., 2015; Pastorello, 2020) and Dorinne (Gourlez De La Motte et al., 2016), demonstrated the model's ability to replicate seasonal and inter-annual carbon dynamics. However, slight GPP overestimations were observed, ranging from 89 g C m^{-2} yr^{-1} in 2014 to 360 g C m^{-2} yr^{-1} in 2013. These discrepancies may result from the model's limited representation of land management practices, such as grazing and fertilization, critical for grassland carbon dynamics.

Additionally, strong correlations (R^2 > 0.75) and low RMSE values for 2020 were observed when comparing AGB estimates with GEDI and ESA-CCI datasets, further reinforcing the model's robustness (Bhan et al., 2021; Roebroek et al., 2023). However, discrepancies in GEDI data, such as the under-representation of understory contributions, underscore the need to integrate multi-layered forest structures in future iterations (Hunka et al., 2023). Overall, the validation demonstrated the CARAIB DVM's effectiveness in simulating carbon fluxes and stocks across diverse spatial and temporal scales. Despite minor discrepancies between satellite and ground-based observations, the strong correlations and consistent trends confirm the model's reliability as a tool for assessing ecosystem carbon dynamics under varying climatic and LULC conditions.

Published in : Journal of Environmental Management (2025), vol. 375, 124329
DOI: 10.1016/j.jenvman.2025.124329
Status : Postprint (Author's version)

OVERALL REGIONAL IMPACT

The findings, supported by detailed validation, highlight the significant role of LULC in carbon dynamics in Wallonia. Grasslands, validated at BE-Dorinne (50.30°N, 4.93°E), exhibited GPP values of 2200-2400 g C m^{-2} yr^{-1} (Gourlez de la Motte et al., 2016), while forests, validated at BE-Vielsalm (50.31°N, 5.99°E), displayed seasonal and interannual GPP variations (Tang et al., 2015). These results estimate Wallonia's annual GPP at 24.302 Mt C from 2001 to 2020, emphasizing the complementary roles of grasslands and forests in carbon assimilation. Grasslands have a strong capacity for carbon sequestration, even under extreme conditions like drought and wildfire, due to their stable belowground carbon storage (Dass et al., 2018). Consistently, grasslands contributed significantly to Wallonia's regional carbon assimilation through high photosynthetic efficiency and extensive root systems.

For forest biomass, the CARAIB DVM estimated a mean carbon stock of 9.55 kg C/m^2, closely matching values from Lettens et al. (2008) and differing by 11% from Vande Walle et al. (2005). These consistent results validate the model while highlighting areas for refinement, particularly in anthropogenic influences and LULC variability (Guo and Gifford, 2002). Collectively, the validated outputs underscore the importance of high-resolution inputs and species-specific traits in capturing regional carbon dynamics and supporting effective land management strategies.

UNCERTAINTY ANALYSIS

The uncertainty analysis highlighted the distinct sensitivity of GPP, NEP, total biomass, and TSC to input parameter variability, providing critical insights into ecosystem processes and model robustness. By incorporating fuzzy membership levels (left, peak, right), we determined how uncertainties in key plant physiological parameters (e.g., SLA, stomatal conductance, and carbon allocation efficiency) propagate through model predictions. GPP exhibited the highest sensitivity to parameter variability, with wide uncertainty ranges observed across fuzzy membership levels. Higher GPP values under left-side memberships reflected favorable assumptions about plant productivity, such as enhanced stomatal conductance and carbon uptake rates. In contrast, right-side memberships constrained GPP predictions, mirroring conservative assumptions.

Published in : Journal of Environmental Management (2025), vol. 375, 124329
DOI: 10.1016/j.jenvman.2025.124329
Status : Postprint (Author's version)

This pronounced sensitivity highlights the influence of short-term physiological processes on productivity and emphasizes the need for better-constrained parameters, such as SLA and stomatal conductance (g_0, g_1), through targeted field measurements. Similarly, NEP displayed significant year-to-year fluctuations, reflecting its dual dependence on both productivity and ecosystem respiration. Left-side memberships led to positive net carbon gains, while right-side memberships approached neutrality or carbon losses, particularly in years of low productivity or increased respiration. These findings underscore NEP's vulnerability to parameter perturbations and the importance of improving model representation of respiration dynamics.

While total biomass was moderately sensitive to parameter variability, it demonstrated greater stability compared to GPP and NEP. The steady increase in total biomass over time, even under varying fuzzy membership levels, indicates that cumulative growth processes are less influenced by short-term uncertainties. Higher total biomass estimates for left-side memberships reflected favorable growth conditions, while right-side memberships constrained accumulation. This stability suggests that total biomass predictions are robust under realistic parameter ranges. In contrast, TSC displayed limited variability across fuzzy membership levels but may strongly depend on historical site management, which is often undocumented. This introduced uncertainty that was not evaluated in our analysis. While TSC buffered short-term fluctuations by integrating long-term carbon inputs, addressing these uncertainties requires improved representation of historical LULC in future studies.

Overall, the analysis highlighted a gradient of sensitivity across ecosystem variables. GPP and NEP exhibited the highest sensitivity to parameter uncertainties, particularly those related to short-term physiological processes such as stomatal conductance and carbon allocation efficiency. Therefore, GPP and NEP were especially vulnerable to input variability. In contrast, total biomass showed moderate sensitivity, reflecting its cumulative growth processes that were less influenced by short-term fluctuations. TSC, on the other hand, remained remarkably stable as a long-term carbon pool, buffering short-term input variability by integrating historical carbon dynamics.

By integrating fuzzy logic and quantifying uncertainty through 90% confidence intervals, this study provides a robust framework for evaluating the impact of input variability on model predictions. These results underscore the need to reduce parameter uncertainties,

Published in : Journal of Environmental Management (2025), vol. 375, 124329
DOI: 10.1016/j.jenvman.2025.124329
Status : Postprint (Author's version)

particularly for sensitive variables like GPP and NEP. Future research should focus on targeted field measurements, improved representation of plant physiological processes, and the incorporation of high-resolution observational datasets to enhance model accuracy and reliability.

IMPLICATIONS OF FUTURE SCENARIOS ON CARBON DYNAMICS

Future simulations under RCP 8.5 and RCP 2.6 underscored the critical influence of LULC change on carbon dynamics, highlighting afforestation, deforestation, and shifts in land-use practices as key factors driving carbon fluxes (GPP, NEP, NBP) and stocks (total biomass and TSC).

IMPLICATIONS OF THE AFFORESTATION AND BAU SCENARIOS

The results underscore the pivotal role of afforestation as a robust strategy to enhance carbon sequestration. Afforestation increased forest GPP, NEP, and total biomass across both climate pathways, reinforcing its potential to offset emissions (Haseeb et al., 2024). These findings align with global mitigation efforts to expand forest cover. In contrast, the BAU scenario, although maintaining moderate productivity, lacked the transformative capacity to significantly enhance carbon storage. Under RCP 8.5, CO_2 fertilization boosted pasture productivity, but this was insufficient to compensate for rising emissions. These results emphasize the need for proactive land management policies beyond current practices.

SCENARIO-BASED SENSITIVITY ANALYSIS: FOREST SHIFT, PARTIAL DEFORESTATION, AND DEFORESTATION

The sensitivity analysis revealed distinct carbon dynamics across LULC scenarios, with notable differences between climate pathways (RCP 2.6 and RCP 8.5). LULC transitions, such as forest shift and deforestation, played a critical role in shaping future carbon fluxes and stocks. In the forest shift scenario, grasslands maintained high productivity under both climate pathways, benefiting from CO_2 fertilization. Initially, the conversion of forests to grasslands enhanced photosynthesis and carbon fixation by remaining vegetation, consistent with previous studies (Prescher et al., 2010). However, from 2046 to 2070, urban expansion significantly altered carbon dynamics, with NEP declining to -12 g C m^{-2} yr^{-1} and NBP dropping to -23 g C m^{-2} yr^{-1}, signaling a shift from carbon sinks to sources.

Published in : Journal of Environmental Management (2025), vol. 375, 124329
DOI: 10.1016/j.jenvman.2025.124329
Status : Postprint (Author's version)

Additionally, this scenario resulted in approximately 25 Mt C less total biomass than the afforestation scenario, although TSC was 4.74% higher, illustrating trade-offs between aboveground and belowground carbon pools.

The partial deforestation scenario exhibited relatively stable GPP trends, with modest increases in forest and pasture productivity. However, carbon loss hotspots emerged in areas of reduced forest cover or intensified urban pressure, particularly under RCP 8.5. In contrast, the deforestation scenario caused the most severe declines, shifting ecosystems from carbon sinks to significant carbon sources. Despite minor gains in pasture GPP, these increases could not compensate for substantial losses in aboveground and belowground carbon stocks.

Overall, while grasslands maintained high productivity, their limited sequestration potential and susceptibility to fragmentation restricted their ability to offset forest carbon losses. The persistence of deforestation hotspots across pathways underscores an urgency for proactive LULC policies, such as forest retention and afforestation, to maintain carbon balances and enhance ecosystem resilience under future climate scenarios.

INSIGHTS FROM CARBON STOCK TRENDS

Total biomass and TSC trends further reinforced the importance of afforestation. Total biomass increased substantially under afforestation, reaching 110 Mt C under RCP 2.6, while it remained stable in the BAU scenario under both climate pathways. TSC showed resilience, maintaining consistent levels across scenarios and pathways, underscoring the long-term stability of belowground carbon pools. However, the deforestation scenario led to significant reductions in total biomass, reflecting the vulnerability of aboveground carbon storage to LULC change. These trends emphasize the dual importance of preserving both aboveground and belowground carbon stocks in climate mitigation strategies.

SPATIAL PATTERNS AND POLICY IMPLICATIONS

Spatial distribution maps revealed significant heterogeneity in carbon fluxes and stocks across LULC scenarios. Afforestation emerged as an effective strategy to mitigate carbon loss hotspots, particularly in southern regions. Conversely, urban- and pasture-dominated areas consistently exhibited persistent carbon losses, underscoring the need for targeted mitigation strategies. The deforestation scenario, on the other hand, led to widespread degradation, emphasizing the urgent need for policy interventions to limit forest-to-urban conversions and

Published in : Journal of Environmental Management (2025), vol. 375, 124329
DOI: 10.1016/j.jenvman.2025.124329
Status : Postprint (Author's version)

promote sustainable transitions. Distinct dynamics between RCP 2.6 and RCP 8.5 in the LULC scenarios highlighted complex interplay between LULC changes and climate change. While afforestation demonstrated substantial potential for enhancing carbon storage (Haseeb et al., 2024), its success depends on complementary land-use policies that address urban expansion and optimize grassland management (Zhao et al., 2023).

LIMITATIONS AND FUTURE DIRECTIONS

We acknowledge several key limitations of the current study. The model lacks a comprehensive integration of carbon–nitrogen interactions, which are important for accurately simulating nutrient dynamics and their influence on ecosystem processes. Additionally, it does not account for critical land management practices (grazing and thinning, planting of new forest or crop species, etc.), limiting its ability to represent nuanced ecosystem processes. In particular, the model does not include thinning, a practice that can have important effects on forest carbon stocks and fluxes. Furthermore, the model does not adequately address the short-term impacts of extreme climate events, such as the effects of storms on forests, which play a significant role in shaping ecosystem carbon dynamics.

Future research should prioritize improving data assimilation techniques and adopting stochastic approaches, such as agent-based modeling combined with high-resolution spatial data, to simulate LULC transitions under varying socio-economic and environmental conditions (Beckers et al., 2018). Incorporating socio-economic drivers, such as afforestation incentives, carbon pricing mechanisms, and urbanization pressures, will address the gap in linking LULC changes to human decision-making processes, enhancing the predictive capability of LULC models. Additionally, collecting data to integrate thinning as a key forest management strategy and advancing uncertainty analysis through the application of type-2 fuzzy logic will strengthen the model's robustness and applicability.

Evaluating ecosystem resilience under extreme events (e.g., droughts, wildfires) and extending the analysis to diverse regions will provide deeper insights into carbon dynamics and ecosystem functioning. These advancements will also inform climate adaptation and mitigation strategies, ensuring the broader applicability of the model in diverse socio-ecological contexts.

Published in : Journal of Environmental Management (2025), vol. 375, 124329
DOI: 10.1016/j.jenvman.2025.124329
Status : Postprint (Author's version)

Conclusion

This study validates the CARAIB DVM's ability to simulate regional carbon dynamics by integrating high-resolution inputs and species-specific traits. Historical simulations confirmed forests as major aboveground carbon sinks and grasslands as contributors to belowground carbon stability. Future projections underscored afforestation as a critical strategy to enhance carbon sequestration, while deforestation under high-emission scenarios transitioned forests from net carbon sinks to sources. Grasslands, although resilient to moderate LULC changes, had limited potential to offset forest carbon losses. Uncertainty analysis revealed the sensitivity of key ecosystem variables, such as GPP and NEP, to plant physiological parameters like stomatal conductance (g0, g1), SLA, and the C:N ratio. Incorporating fuzzy logic quantified parameter variability and strengthened the reliability of future projections.

We identified actionable outcomes from our findings. Policymakers must prioritize afforestation programs in regions with high sequestration potential while enforcing stricter regulations to limit deforestation, particularly in areas at risk of urban expansion. Additionally, sustainable grassland management should be incentivized through subsidies or carbon credit systems, recognizing the role of grasslands in belowground carbon storage. Investments in advanced monitoring systems and targeted field studies are essential to refine parameter accuracy and strengthen future LULC planning. These recommendations provide a clear roadmap for enhancing ecosystem resilience and achieving climate mitigation goals under changing climatic conditions.

CRediT authorship contribution statement

Arpita Verma: Writing – original draft, Visualization, Validation, Methodology, Investigation, Funding acquisition, Formal analysis, Data curation, Conceptualization. **Benjamin Lanssens:** Writing - review & editing, Data curation. **Merja Tölle:** Writing - review & editing, Data curation. **Ingrid Jacquemin:** Writing – original draft, Data curation. **Tarunsinh Chaudhari:** Writing - review & editing, Data curation. **Alain Hambuckers:** Writing - review & editing. **Louis François:** Writing - review & editing, Supervision, Project administration, Funding acquisition.

Funding

This work was generously supported by the FNRS – FRIA fellowship (A. Verma; Grant number: FC 36,319), providing essential resources for our research. This work also has been conducted

Published in : Journal of Environmental Management (2025), vol. 375, 124329
DOI: 10.1016/j.jenvman.2025.124329
Status : Postprint (Author's version)

within the MAPPY project (Multisectoral analysis of climate and land use change impacts on pollinators, plant diversity and crop yields) which is part of AXIS, an ERA-NET initiated by JPI Climate, and funded in the French-speaking part of Belgium by F.R.S.-FNRS (B. Lanssens, I. Jacquemin & L. François; Grant number: R.8003.19) and in Germany by DLR/BMBF (M. Tolle; Grant number: 776,608, Funding reference No. 01LS1903C).

DECLARATION OF COMPETING INTEREST

The authors declare the following financial interests/personal relationships which may be considered as potential competing interests: Arpita Verma reports financial support was provided by Fund for Scientific Research-FRIA. Louis François reports financial support was provided by Fund for Scientific Research -FRS-FNRS. Benjamin Lanssens reports financial support was provided by Fund for Scientific Research -FRS-FNRS. There is no conflict of interest with co-authors. If there are other authors, they declare that they have no known competing financial interests or personal relationships that could have appeared to influence the work reported in this paper.

APPENDIX A. SUPPLEMENTARY DATA

Supplementary data to this article can be found online at https://doi.org/10.1016/j.jenvman.2025.124329.

List of Abbreviations	
AGB	Aboveground Biomass
BAG	Bioclimatic Affinity Groups
BAU	Business As Usual
CARAIB	CARbon Assimilation In the Biosphere
CORINE	Coordination of Information on the Environment
COSMO	Consortium for Small-Scale Modeling
CO2	Carbon Dioxide
CLM	Climate Limited-Area Modeling
DVM	Dynamic Vegetation Model

Published in : Journal of Environmental Management (2025), vol. 375, 124329
DOI: 10.1016/j.jenvman.2025.124329
Status : Postprint (Author's version)

ESA-CCI	European Space Agency Climate Change Initiative
FAPAR	Fraction of Absorbed Photosynthetically Active Radiation
GPP	Gross Primary Productivity
GEE	Google Earth Engine
GEDI	Global Ecosystem Dynamics investigation
GWR	Geographical Weighted Regression
GSWP3	Global Soil Wetness Project Phase 3
HWSD	Harmonized World Soil Database
LULC	Land Use/Land Cover
ML	Machine Learning
MODIS	Moderate Resolution Imaging Spectroradiometer
NPP	Net Primary Productivity
NEP	Net Ecosystem Productivity
NBP	Net Biome Productivity
PFT	Plant Functional Type
RF	Random Forest
RCP	Representative Concentration Pathways
SVM	Support Vector Machine
SLA	Specific Leaf Area
TFNs	Triangular Fuzzy Numbers

DATA AVAILABILITY

Data will be made available on request.

Published in : Journal of Environmental Management (2025), vol. 375, 124329
DOI: 10.1016/j.jenvman.2025.124329
Status : Postprint (Author's version)

References

Amani, M., Ghorbanian, A., Ahmadi, S.A., Kakooei, M., Moghimi, A., Mirmazloumi, S.M., Moghaddam, S.H.A., Mahdavi, S., Ghahremanloo, M., Parsian, S., Wu, Q., Brisco, B., 2020. Google Earth Engine cloud computing platform for remote sensing big data applications: a comprehensive review. IEEE J. Sel. Top. Appl. Earth Observations Remote Sensing 13, 5326–5350. https://doi.org/10.1109/JSTARS.2020.3021052.

Augusto, L., Boča, A., 2022. Tree functional traits, forest biomass, and tree species diversity interact with site properties to drive forest soil carbon. Nat. Commun. 13, 1097. https://doi.org/10.1038/s41467-022-28748-0.

Ball, J.T., Woodrow, I.E., Berry, J.A., 1987. A model predicting stomatal conductance and its contribution to the control of photosynthesis under different environmental conditions. In: Biggins, J. (Ed.), Progress in Photosynthesis Research. Springer, Netherlands, Dordrecht, pp. 221–224. https://doi.org/10.1007/978-94-017-0519-6_ 48.

Bastos, A., O'Sullivan, M., Ciais, P., Makowski, D., Sitch, S., Friedlingstein, P., Chevallier, F., Rödenbeck, C., Pongratz, J., Luijkx, I.T., Patra, P.K., Peylin, P., Canadell, J.G., Lauerwald, R., Li, W., Smith, N.E., Peters, W., Goll, D.S., Jain, A.K., Kato, E., Lienert, S., Lombardozzi, D.L., Haverd, V., Nabel, J.E.M.S., Poulter, B., Tian, H., Walker, A.P., Zaehle, S., 2020. Sources of uncertainty in regional and global terrestrial CO_2 exchange estimates. Global Biogeochem. Cycles 34, e2019GB006393. https://doi.org/10.1029/2019GB006393.

Beckers, V., Beckers, J., Vanmaercke, M., Van Hecke, E., Van Rompaey, A., Dendoncker, N., 2018. Modelling farm growth and its impact on agricultural land use: a country scale application of an agent-based model. Land 7, 109. https://doi. org/10.3390/land7030109.

Bian, C., Xia, J., 2023. Uncertainty propagation in a global biogeochemical model driven by leaf area data. Front. Ecol. Evol. 11, 1105832. https://doi.org/10.3389/ fevo.2023.1105832.

Bhan, M., Gingrich, S., Roux, N., Le Noë, J., Kastner, T., Matej, S., Schwarzmueller, F., Erb, K.-H., 2021. Quantifying and attributing land use-induced carbon emissions to biomass consumption: a critical assessment of existing approaches. J. Environ. Manag. 286, 112228. https://doi.org/10.1016/j.jenvman.2021.112228.

Bultan, S., Nabel, J.E.M.S., Hartung, K., Ganzenmüller, R., Xu, L., Saatchi, S., Pongratz, J., 2022. Tracking 21st century anthropogenic and natural carbon fluxes through model-data integration. Nat. Commun. 13, 5516. https://doi.org/10.1038/ s41467-022-32456-0.

Cai, W., Prentice, I.C., 2020. Recent trends in gross primary production and their drivers: analysis and modelling at flux-site and global scales. Environ. Res. Lett. 15, 124050. https://doi.org/10.1088/1748-9326/abc64e.

Dass, P., Houlton, B.Z., Wang, Y., Warlind, D., 2018. Grasslands may be more reliable carbon sinks than forests in California. Environ. Res. Lett. 13, 074027. https://doi. org/10.1088/1748-9326/aacb39.

Published in : Journal of Environmental Management (2025), vol. 375, 124329
DOI: 10.1016/j.jenvman.2025.124329
Status : Postprint (Author's version)

De Wergifosse, L., André, F., Goosse, H., Caluwaerts, S., De Cruz, L., De Troch, R., Van Schaeybroeck, B., Jonard, M., 2020. CO_2 fertilization, transpiration deficit and vegetation period drive the response of mixed broadleaved forests to a changing climate in Wallonia. Ann. For. Sci. 77, 70. https://doi.org/10.1007/s13595-020- 00966-w.

Dury, M., Hambuckers, A., Warnant, P., Henrot, A., Favre, E., Ouberdous, M., François, L., 2011. Responses of European forest ecosystems to 21st century climate: assessing changes in interannual variability and fire intensity. iForest 4, 82–99. https://doi.org/10.3832/ifor0572-004.

Dury, M., Mertens, L., Fayolle, A., Verbeeck, H., Hambuckers, A., François, L., 2018. Refining species traits in a dynamic vegetation model to project the impacts of climate change on tropical trees in Central Africa. Forests 9, 722. https://doi.org/ 10.3390/f9110722.

Duncanson, L., Armston, J., Disney, M., Avitabile, V., Barbier, N., Calders, K., Carter, S., Chave, J., Herold, M., Crowther, T.W., Falkowski, M., Kellner, J.R., Labrière, N., Lucas, R., MacBean, N., McRoberts, R.E., Meyer, V., Næsset, E., Nickeson, J.E., Paul, K.I., Phillips, O.L., Réjou-Méchain, M., Roman, M., Roxburgh, S., Saatchi, S., Schepaschenko, D., Scipal, K., Siqueira, P.R., Whitehurst, A., Williams, M., 2019. The importance of consistent global forest aboveground biomass product validation. Surv. Geophys. 40, 979–999. https://doi.org/10.1007/s10712-019-09538-8.

Farquhar, G.D., von Caemmerer, S., Berry, J.A., 1980. A biochemical model of photosynthetic CO2 assimilation in leaves of C3 species. Planta 149, 78–90. https:// doi.org/10.1007/BF00386231.

Friedlingstein, P., O'Sullivan, M., Jones, M.W., Andrew, R.M., Bakker, D.C.E., Hauck, J., Landschützer, P., Le Quéré, C., Luijkx, I.T., Peters, G.P., Peters, W., Pongratz, J., Schwingshackl, C., Sitch, S., Canadell, J.G., Ciais, P., Jackson, R.B., Alin, S.R., Anthoni, P., Barbero, L., Bates, N.R., Becker, M., Bellouin, N., Decharme, B., Bopp, L., Brasika, I.B.M., Cadule, P., Chamberlain, M.A., Chandra, N., Chau, T.-T.-T., Chevallier, F., Chini, L.P., Cronin, M., Dou, X., Enyo, K., Evans, W., Falk, S., Feely, R. A., Feng, L., Ford, D.J., Gasser, T., Ghattas, J., Gkritzalis, T., Grassi, G., Gregor, L., Gruber, N., Gürses, Ö., Harris, I., Hefner, M., Heinke, J., Houghton, R.A., Hurtt, G.C., Iida, Y., Ilyina, T., Jacobson, A.R., Jain, A., Jarniková, T., Jersild, A., Jiang, F., Jin, Z., Joos, F., Kato, E., Keeling, R.F., Kennedy, D., Klein Goldewijk, K., Knauer, J., Korsbakken, J.I., Körtzinger, A., Lan, X., Lefèvre, N., Li, H., Liu, J., Liu, Z., Ma, L., Marland, G., Mayot, N., McGuire, P.C., McKinley, G.A., Meyer, G., Morgan, E.J., Munro, D.R., Nakaoka, S.-I., Niwa, Y., O'Brien, K.M., Olsen, A., Omar, A.M., Ono, T., Paulsen, M., Pierrot, D., Pocock, K., Poulter, B., Powis, C.M., Rehder, G., Resplandy, L., Robertson, E., Rödenbeck, C., Rosan, T.M., Schwinger, J., Séférian, R., Smallman, T.L., Smith, S.M., Sospedra-Alfonso, R., Sun, Q., Sutton, A.J., Sweeney, C., Takao, S., Tans, P.P., Tian, H., Tilbrook, B., Tsujino, H., Tubiello, F., Van Der Werf, G.R., Van Ooijen, E., Wanninkhof, R., Watanabe, M., Wimart-Rousseau, C., Yang, D., Yang, X., Yuan, W., Yue, X., Zaehle, S., Zeng, J., Zheng, B., 2023. Global carbon budget 2023. Earth Syst. Sci. Data 15, 5301–5369. https://doi.org/10.5194/ essd-15-5301-2023.

Published in : Journal of Environmental Management (2025), vol. 375, 124329
DOI: 10.1016/j.jenvman.2025.124329
Status : Postprint (Author's version)

François, L.M., Goddéris, Y., Warnant, P., Ramstein, G., de Noblet, N., Lorenz, S., 1999. Carbon stocks and isotopic budgets of the terrestrial biosphere at mid-Holocene and last glacial maximum times. Chem. Geol. 159, 163–189. https://doi.org/10.1016/ S0009-2541(99)00039-X.

François, L., Utescher, T., Favre, E., Henrot, A.-J., Warnant, P., Micheels, A., Erdei, B., Suc, J.-P., Cheddadi, R., Mosbrugger, V., 2011. Modelling Late Miocene vegetation in Europe: results of the CARAIB model and comparison with palaeovegetation data. Palaeogeogr. Palaeoclimatol. Palaeoecol. 304, 359–378. https://doi.org/10.1016/j. palaeo.2011.01.012.

García-Álvarez, D., Camacho Olmedo, M.T., Paegelow, M., Mas, J.F. (Eds.), 2022. Land Use Cover Datasets and Validation Tools: Validation Practices with QGIS. Springer International Publishing, Cham. https://doi.org/10.1007/978-3-030-90998-7.

Gérard, J.C., Nemry, B., François, L.M., Warnant, P., 1999. The interannual change of atmospheric CO_2: Contribution of subtropical ecosystems. Geophys. Res. Lett. 26, 243–246. https://doi.org/10.1029/1998GL900269.

Gorelick, N., Hancher, M., Dixon, M., Ilyushchenko, S., Thau, D., Moore, R., 2017. Google Earth engine: planetary-scale geospatial analysis for everyone. Remote Sensing of Environment 202, 18–27. https://doi.org/10.1016/j.rse.2017.06.031.

Gourlez De La Motte, L., Jérôme, E., Mamadou, O., Beckers, Y., Bodson, B., Heinesch, B., Aubinet, M., 2016. Carbon balance of an intensively grazed permanent grassland in southern Belgium. Agric. For. Meteorol. 228–229, 370–383. https://doi.org/ 10.1016/j.agrformet.2016.06.009.

Guo, L.B., Gifford, R.M., 2002. Soil carbon stocks and land use change: a meta analysis. Global Change Biol. 8, 345–360. https://doi.org/10.1046/j.1354-1013.2002.00486. x.

Hambuckers, A., Trolliet, F., Dury, M., Henrot, A.-J., Porteman, K., El Hasnaoui, Y., Van Den Bulcke, J., De Mil, T., Remy, C.C., Cheddadi, R., François, L., 2022. Towards a more realistic simulation of plant species with a dynamic vegetation model using field-measured traits: the atlas cedar, a case study. Forests 13, 446. https://doi.org/ 10.3390/f13030446.

Hari, M., Tyagi, B., 2022. Terrestrial carbon cycle: tipping edge of climate change between the atmosphere and biosphere ecosystems. Environ. Sci.: Atmos. 2, 867–890. https://doi.org/10.1039/D1EA00102G.

Haseeb, M., Tahir, Z., Mehmood, S.A., Gill, S.A., Farooq, N., Butt, H., Iftikhar, A., Maqsood, A., Abdullah-Al-Wadud, M., Tariq, A., 2024. Enhancing carbon sequestration through afforestation: evaluating the impact of land use and cover

changes on carbon storage dynamics. Earth Syst. Environ. https://doi.org/10.1007/ s41748-024-00414-z.

Henrot, A.-J., Utescher, T., Erdei, B., Dury, M., Hamon, N., Ramstein, G., Krapp, M., Herold, N., Goldner, A., Favre, E., Munhoven, G., François, L., 2017. Middle Miocene climate and

vegetation models and their validation with proxy data. Palaeogeogr. Palaeoclimatol. Palaeoecol. 467, 95–119. https://doi.org/10.1016/j. palaeo.2016.05.026.

Hong, C., Burney, J.A., Pongratz, J., Nabel, J.E.M.S., Mueller, N.D., Jackson, R.B., Davis, S.J., 2021. Global and regional drivers of land-use emissions in 1961–2017. Nature 589, 554–561. https://doi.org/10.1038/s41586-020-03138-y.

Houghton, R.A., 2020. Terrestrial fluxes of carbon in GCP carbon budgets. Glob. Change Biol. 26, 3006–3014. https://doi.org/10.1111/gcb.15050.

Hu, X., He, Y., Kong, Z., Zhang, J., Yuan, M., Yu, L., Peng, C., Zhu, Q., 2021. Evaluation of future impacts of climate change, CO2, and land use cover change on global net primary productivity using a processed model. Land 10, 365. https://doi.org/ 10.3390/land10040365.

Hubert, B., Francois, L., Warnant, P., Strivay, D., 1998. Stochastic generation of meteorological variables and effects on global models of water and carbon cycles in vegetation and soils. J. Hydrol. 212–213, 318–334. https://doi.org/10.1016/S0022-1694(98)00214-5.

Hunka, N., Santoro, M., Armston, J., Dubayah, R., McRoberts, R.E., Næsset, E., Quegan, S., Urbazaev, M., Pascual, A., May, P.B., Minor, D., Leitold, V., Basak, P., Liang, M., Melo, J., Herold, M., Málaga, N., Wilson, S., Durán Montesinos, P., Arana, A., Ernesto De La Cruz Paiva, R., Ferrand, J., Keoka, S., Guerra-Hernández, J., Duncanson, L., 2023. On the NASA GEDI and ESA CCI biomass maps: aligning for uptake in the UNFCCC global stocktake. Environ. Res. Lett. 18, 124042. https://doi. org/10.1088/1748-9326/ad0b60.

Jacquemin, I., Berckmans, J., Henrot, A.-J., Dury, M., Tychon, B., Hambuckers, A., Hamdi, R., François, L., 2020. Using the CARAIB dynamic vegetation model to simulate crop yields in Belgium - validation and projections for the 2035 horizon. Geo-Eco-Trop 44, 541–552.

Journée, M., Bertrand, C., 2011. Geostatistical merging of ground-based and satellite-derived data of surface solar radiation. Adv. Sci. Res. 6, 1–5. https://doi.org/ 10.5194/asr-6-1-2011.

Journée, M., Goudenhoofdt, E., Vannitsem, S., Delobbe, L., 2023. Quantitative rainfall analysis of the 2021 mid-July flood event in Belgium. Hydrol. Earth Syst. Sci. 27, 3169–3189. https://doi.org/10.5194/hess-27-3169-2023.

Junttila, V., Minunno, F., Peltoniemi, M., Forsius, M., Akujärvi, A., Ojanen, P., Makela, A., 2023. Quantification of forest carbon flux and stock uncertainties under climate change and their use in regionally explicit decision making: case study in Finland. Ambio 52, 1716–1733. https://doi.org/10.1007/s13280-023-01906-4.

Jian, J., Bailey, V., Dorheim, K., Konings, A.G., Hao, D., Shiklomanov, A.N., Snyder, A., Steele, M., Teramoto, M., Vargas, R., Bond-Lamberty, B., 2022. Historically inconsistent productivity and respiration fluxes in the global terrestrial carbon cycle. Nat. Commun. 13, 1733. https://doi.org/10.1038/s41467-022-29391-5.

Published in : Journal of Environmental Management (2025), vol. 375, 124329
DOI: 10.1016/j.jenvman.2025.124329
Status : Postprint (Author's version)

Kattge, J., Bönisch, G., Díaz, S., Lavorel, S., Prentice, I.C., Leadley, P., et al., 2020. TRY plant trait database – enhanced coverage and open access. Global Change Biol. 26, 119–188. https://doi.org/10.1111/gcb.14904.

Keenan, T.F., Williams, C.A., 2018. The terrestrial carbon sink. Annu. Rev. Environ. Resour. 43, 219–243. https://doi.org/10.1146/annurev-environ-102017-030204.

Kong, R., Zhang, Z., Huang, R., Tian, J., Feng, R., Chen, X., 2022. Projected global warming-induced terrestrial ecosystem carbon across China under SSP scenarios. Ecol. Indicat. 139, 108963. https://doi.org/10.1016/j.ecolind.2022.108963.

Krause, A., Papastefanou, P., Gregor, K., Layritz, L.S., Zang, C.S., Buras, A., Li, X., Xiao, J., Rammig, A., 2022. Quantifying the impacts of land cover change on gross primary productivity globally. Sci. Rep. 12, 18398. https://doi.org/10.1038/ s41598-022-23120-0.

Latte, N., Colinet, G., Fayolle, A., Lejeune, P., Hébert, J., Claessens, H., Bauwens, S., 2013. Description of a new procedure to estimate the carbon stocks of all forest pools and impact assessment of methodological choices on the estimates. Eur. J. Forest Res. 132, 565–577. https://doi.org/10.1007/s10342-013-0701-6.

Lettens, S., Orshoven, J., Wesemael, B., Muys, B., Perrin, D., 2005. Soil organic carbon changes in landscape units of Belgium between 1960 and 2000 with reference to 1990. Global Change Biol. 11, 2128–2140. https://doi.org/10.1111/j.1365- 2486.2005.001074.x.

Lettens, S., Van Orshoven, J., Perrtn, D., Van Wesemael, B., Muys, B., 2008. Organic carbon stocks and stock changes of forest biomass in Belgium derived from forest inventory data in a spatially explicit approach. Ann. For. Sci. 65. https://doi.org/ 10.1051/forest:2008034, 604–604.

Li, W., MacBean, N., Ciais, P., Defourny, P., Lamarche, C., Bontemps, S., Houghton, R.A., Peng, S., 2018. Gross and net land cover changes in the main plant functional types derived from the annual ESA CCI land cover maps (1992–2015). Earth Syst. Sci. Data 10, 219–234. https://doi.org/10.5194/essd-10-219-2018.

Li, Xiao, 2019. Mapping photosynthesis solely from solar-induced chlorophyll fluorescence: a global, fine-resolution dataset of gross primary production derived from OCO-2. Rem. Sens. 11, 2563. https://doi.org/10.3390/rs11212563.

Li, X., Ma, H., Ran, Y., Wang, X., Zhu, G., Liu, F., He, H., Zhang, Z., Huang, C., 2021. Terrestrial carbon cycle model-data fusion: progress and challenges. Sci. China Earth Sci. 64, 1645–1657. https://doi.org/10.1007/s11430-020-9800-3.

Loudiyi, I., Jacquemin, I., Lahlou, M., Balaghi, R., Tychon, B., François, L., 2024. Atmospheric CO2 fertilization effect on cereal yields in Morocco using the CARAIB dynamic vegetation model. Eur. J. Agron. 161, 127374. https://doi.org/10.1016/j. eja.2024.127374.

Published in : Journal of Environmental Management (2025), vol. 375, 124329
DOI: 10.1016/j.jenvman.2025.124329
Status : Postprint (Author's version)

Miner, G.L., Bauerle, W.L., Baldocchi, D.D., 2017. Estimating the sensitivity of stomatal conductance to photosynthesis: a review. Plant Cell Environ. 40, 1214–1238. https://doi.org/10.1111/pce.12871.

McGlynn, E., Li, S., F Berger, M., Amend, M., L Harper, K., 2022. Addressing uncertainty and bias in land use, land use change, and forestry greenhouse gas inventories. Climatic Change 170, 5. https://doi.org/10.1007/s10584-021-03254-2.

Meinshausen, M., Smith, S.J., Calvin, K., Daniel, J.S., Kainuma, M.L.T., Lamarque, J.-F., Matsumoto, K., Montzka, S.A., Raper, S.C.B., Riahi, K., Thomson, A., Velders, G.J.M., Van Vuuren, D.P.P., 2011. The RCP greenhouse gas concentrations and their extensions from 1765 to 2300. Climatic Change 109, 213–241. https://doi.org/ 10.1007/s10584-011-0156-z.

O'Sullivan, M., Friedlingstein, P., Sitch, S., Anthoni, P., Arneth, A., Arora, V.K., Bastrikov, V., Delire, C., Goll, D.S., Jain, A., Kato, E., Kennedy, D., Knauer, J., Lienert, S., Lombardozzi, D., McGuire, P.C., Melton, J.R., Nabel, J.E.M.S., Pongratz, J., Poulter, B., Seferian, R., Tian, H., Vuichard, N., Walker, A.P., Yuan, W., Yue, X., Zaehle, S., 2022. Process-oriented analysis of dominant sources of uncertainty in the land carbon sink. Nat. Commun. 13, 4781. https://doi.org/ 10.1038/s41467-022-32416-8.

Pastorello, G., 2020. The FLUXNET2015 Dataset and the ONEFlux Processing Pipeline for Eddy Covariance Data, vol. 7, p. 225. https://doi.org/10.1038/s41597-020-0534-3.

Phan, T.N., Kuch, V., Lehnert, L.W., 2020. Land cover classification using Google Earth Engine and Random Forest classifier—the role of image composition. Rem. Sens. 12, 2411. https://doi.org/10.3390/rs12152411.

Pongratz, J., Schwingshackl, C., Bultan, S., Obermeier, W., Havermann, F., Guo, S., 2021. Land use effects on climate: current state, recent progress, and emerging topics. Curr. Clim. Change Rep. 7, 99–120. https://doi.org/10.1007/s40641-021-00178-y.

Prescher, A.-K., Grünwald, T., Bernhofer, C., 2010. Land use regulates carbon budgets in eastern Germany: from NEE to NBP. Agric. For. Meteorol. 150, 1016–1025. https://doi.org/10.1016/j.agrformet.2010.03.008.

Roebroek, C.T.J., Duveiller, G., Seneviratne, S.I., Davin, E.L., Cescatti, A., 2023. Releasing global forests from human management: how much more carbon could be stored? Science 380, 749–753. https://doi.org/10.1126/science.add5878.

Rojas-Botero, S., Teixeira, L.H., Prucker, P., Kloska, V., Kollmann, J., Le Stradic, S., 2023. Root traits of grasslands rapidly respond to climate change, while community biomass mainly depends on functional composition. Funct. Ecol. 37, 1841–1855. https://doi.org/10.1111/1365-2435.14345.

Sun, Y., Frankenberg, C., Wood, J.D., Schimel, D.S., Jung, M., Guanter, L., Drewry, D.T., Verma, M., Porcar-Castell, A., Griffis, T.J., Gu, L., Magney, T.S., Kohler, P., Evans, B., Yuen, K., 2017. OCO-2 advances photosynthesis observation from space via solar- induced chlorophyll fluorescence. Science 358, eaam5747. https://doi.org/ 10.1126/science.aam5747.

Published in : Journal of Environmental Management (2025), vol. 375, 124329
DOI: 10.1016/j.jenvman.2025.124329
Status : Postprint (Author's version)

Tang, X., Li, H., Huang, N., Li, X., Xu, X., Ding, Z., Xie, J., 2015. A comprehensive assessment of MODIS-derived GPP for forest ecosystems using the site-level FLUXNET database. Environ. Earth Sci. 74, 5907–5918. https://doi.org/10.1007/ s12665-015-4615-0.

Trugman, A.T., Quetin, G.R., 2023. Leveraging uncertainty in terrestrial ecosystem carbon stocks and fluxes. Earth's Future 11, e2022EF003322. https://doi.org/ 10.1029/2022EF003322.

Vande Walle, I., Van Camp, N., Perrin, D., Lemeur, R., Verheyen, K., Van Wesemael, B., Laitat, E., 2005. Growing stock-based assessment of the carbon stock in the Belgian forest biomass. Ann. For. Sci 62, 853–864. https://doi.org/10.1051/forest:2005076.

Warnant, P., Francois, L., Strivay, D., Gerard, J.-C., 1994. CARAIB: a global model of terrestrial biological productivity. Global Biogeochem. Cycles 8, 255–270. https:// doi.org/10.1029/94GB00850.

Yang, Y., Zhao, J., Zhao, P., Wang, H., Wang, B., Su, S., Li, M., Wang, L., Zhu, Q., Pang, Z., Peng, C., 2019. Trait-based climate change predictions of vegetation sensitivity and distribution in China. Front. Plant Sci. 10, 908. https://doi.org/ 10.3389/fpls.2019.00908.

Yuh, Y.G., Tracz, W., Matthews, H.D., Turner, S.E., 2023. Application of machine learning approaches for land cover monitoring in northern Cameroon. Ecol. Inf. 74, 101955. https://doi.org/10.1016/j.ecoinf.2022.101955.

Zakharova, L., Meyer, K.M., Seifan, M., 2019. Trait-based modelling in ecology: a review of two decades of research. Ecol. Model. 407, 108703. https://doi.org/10.1016/j. ecolmodel.2019.05.008.

Zhao, G., Liu, L., Wang, Z.-Y., Jin, Z., He, J.-S., 2023. Grassland science in a new era. Fundamental Research 3, 149–150. https://doi.org/10.1016/j.fmre.2023.02.001.

Zhou, Y., Chartin, C., Van Oost, K., Van Wesemael, B., 2022. High-resolution soil organic carbon mapping at the field scale in Southern Belgium (Wallonia). Geoderma 422, 115929. https://doi.org/10.1016/j.geoderma.2022.115929.